PRESSURISATION AND BRINE DISPLACEMENT ISSUES FOR DEEP SALINE FORMATION CO_2 STORAGE

Report: 2010/15

November 2010

INTERNATIONAL ENERGY AGENCY

The International Energy Agency (IEA) was established in 1974 within the framework of the Organisation for Economic Co-operation and Development (OECD) to implement an international energy programme. The IEA fosters co-operation amongst its 28 member countries and the European Commission, and with the other countries, in order to increase energy security by improved efficiency of energy use, development of alternative energy sources and research, development and demonstration on matters of energy supply and use. This is achieved through a series of collaborative activities, organised under more than 40 Implementing Agreements. These agreements cover more than 200 individual items of research, development and demonstration. IEAGHG is one of these Implementing Agreements.

DISCLAIMER

This report was prepared as an account of the work sponsored by IEAGHG. The views and opinions of the authors expressed herein do not necessarily reflect those of the IEAGHG, its members, the International Energy Agency, the organisations listed below, nor any employee or persons acting on behalf of any of them. In addition, none of these make any warranty, express or implied, assumes any liability or responsibility for the accuracy, completeness or usefulness of any information, apparatus, product of process disclosed or represents that its use would not infringe privately owned rights, including any parties intellectual property rights. Reference herein to any commercial product, process, service or trade name, trade mark or manufacturer does not necessarily constitute or imply any endorsement, recommendation or any favouring of such products.

COPYRIGHT

ACKNOWLEDGEMENTS AND CITATIONS

This report describes research sponsored by IEAGHG. This report was prepared by:

The Permedia Research Group

The principal researchers were:

- Andrew Cavanagh, PhD

To ensure the quality and technical integrity of the research undertaken by IEAGHG each study is managed by an appointed IEAGHG manager. The report is also reviewed by a panel of independent technical experts before its release.

The IEAGHG manager for this report was:

- Neil Wildgust

The expert reviewers for this report were:

- Stefan Bachu, Alberta Innovates – Technology Futures
- Andy Chadwick, BGS
- John Wilkinson, ExxonMobil
- Gary Teletzke, ExxonMobil
- Stephen Cawley, BP Alternative Energy
- Erik Nygaard, GEUS
- Yann le Gallo, Geogreen

The report should be cited in literature as follows:

'IEAGHG, "Pressurisation and Brine Displacement Issues for Deep Saline Formation CO_2 Storage", 2010/15, November, 2010.'

Further information or copies of the report can be obtained by contacting IEAGHG at:

IEAGHG, Orchard Business Centre,
Stoke Orchard, Cheltenham,
GLOS., GL52 7RZ, UK
Tel: +44(0) 1242 680753 Fax: +44 (0)1242 680758
E-mail: mail@ieaghg.org
Internet: www.ieaghg.org

PRESSURISATION AND BRINE DISPLACEMENT ISSUES FOR DEEP SALINE FORMATION CO_2 STORAGE

Background to the Study

Deep saline formations (DSF) are widely considered to offer the largest potential capacity for the geological storage of carbon dioxide (CO_2) as a greenhouse gas mitigation option. Whilst storage in DSF has already been demonstrated as a viable technological option (e.g. Sleipner, In-Salah), discussions at the GHGT9 conference in Washington highlighted an area of significant uncertainty, namely the effects of injecting CO2 into DSF in terms of brine and pressure displacement, particularly where multiple injection schemes may be planned within a formation**.**

Potential problems of over-pressurisation, leading to caprock failures and leakage, or large scale displacement of brine (either through engineered systems or uncontrolled migration), could have a major impact on the viability and implementation of large scale CO_2 storage in DSF. The degree to which brine and pressure displacement occur will be governed by several factors. Key amongst these will be the boundary conditions to the formations into which CO_2 is injected – whether the system is 'open' whereby fluid and pressure communication through the storage formation is strong, or 'closed' where compartmentalisation of the formation by lateral flow boundaries (e.g. faults) effectively limits fluid movement and pressure dissipation. In reality, some systems could actually be regarded as 'semi-closed', with intermediate fluid and pressure communication.

For closed systems, CO_2 injection would result in pressure increase, limiting effective storage capacity to the volume created by both the compressibility of the formation and existing pore fluids, and the limit of pressure increase before physical damage to the system. In contrast, many studies of storage capacity have assumed that open systems will act as 'infinite' formations, where migration of displaced fluids and dissipation of pressure will allow CO_2 injection to progress smoothly. However, this assumption is the source of considerable debate, particularly where formations may be subject to multiple injection schemes, bringing into play the possibility of pressure field interference between injection projects.

The Permedia Research Group, based in Ottawa, Canada was commissioned by IEAGHG in October 2010, to undertake a study aiming to produce a 'high level' overview of long term pressurisation and brine displacement issues. The study will also aimed to highlight the current state of knowledge and / or gaps and recommend further research priorities on these topics.

Scope of Work

This study examined the issues of brine and pressure displacement in detail, firstly through a review of existing information and published studies. The review included data and analysis of actual CO_2 injection projects being undertaken in DSF around the world.

Secondly, the study undertook modelling to facilitate analysis of key topics:

- The importance of storage formation characteristics, relative and absolute permeability variations, compressibility, fracture pressures, heterogeneity – and in particular the likely presence or absence of 'compartmentalisation' in typical regional settings
- Interaction of pressure fields from multiple injection scenarios and evolution of pressure fields with time – an important element of risk profiles
- Pressure effects on caprock and fault integrity
- Potential magnitude and consequences of brine displacement
- Possible engineered solutions e.g. brine extraction

The study was not required to include a detailed assessment of the potential impacts of brine displacement and pressurisation on shallow groundwater resources or other environmental receptors – these topics will be addressed by separate IEAGHG studies (see below).

Permedia was asked to refer to the following recent or ongoing IEAGHG reports/studies relevant to this study, to avoid obvious duplication of effort and to ensure that the reports issued by the programme provide a reasonably coherent output:

- Development Issues for Saline Aquifer Storage, CO2CRC, IEAGHG Report 2008/12.
- Storage Capacity Coefficients, EERC, IEAGHG Report 2009/13.
- Injection Strategies for Storage Sites, CO2CRC, IEAGHG Report 2010/04..
- Impacts on Groundwater Resources, CO2GeoNet, project commenced March 2010.
- Caprock Systems for CO2 Storage, CO2CRC, project commenced April 2010.

Findings of the Study

Introduction and Previous Research

Current debates on storage capacity and injectivity for CO_2 geological storage in DSF largely revolve around the issue of pressurisation, which will be partly governed by the rate at which storage formation brines can migrate away from the storage site. The technical challenges associated with understanding these issues are driven by limited operational experience of large scale DSF storage and the current paucity of characterisation data for many DSF and associated caprocks. Of particular concern for pressurisation effects is the setting of realistic boundary conditions for predictive models.

The fundamental challenge in assigning boundary conditions for models, in the absence of characterisation data and widespread operational experience, is to estimate the permeability of lateral and vertical boundaries to the storage site. In the extreme case, assumptions of compartmentalised storage formations with relatively impermeable boundaries lead to pessimistic calculations of rapid pressure increase and loss of injectivity. In contrast, boundaries of sufficient permeability to allow significant brine migration will serve to restrict pressure increases; however as permeability of shale increases, so will the possibility that CO_2 could also migrate from the storage formation.

Table 1 below summarises the approach taken by selected recent authors in setting boundary conditions for CO_2 geological storage:

Table 1: Summary of System Boundary Conditions

System boundaries	*Brine flux and pressure response*	*Recently published examples*
Open system	Regional lateral flux; transient local pressurisation.	Doughty & Preuss, 2004; USDOE, 2008; Chadwick *et al.*, 2009.
Semi-closed system	Flux at boundaries; moderate regional pressurisation.	Zhou et al., 2008; Thibeau & Mucha, 2009; Holloway *et al.*, 2009.
Closed-system	Flux limited to storage formation; rapid loss of injectivity.	van der Meer & van Wees, 2006; Ehlig-Economides & Economides, 2010.

The report notes that dissolution of CO_2 into formation brine will alleviate pressure build-up; however the proportion of injected CO_2 that will dissolve in residual brine within the CO_2 plume is likely to be relatively modest at 2% or less; therefore any significant contribution to pressure relief would rely on more widespread dissolution in the storage formation. Many authors have cited density-driven convection as a major process to enhance dissolution but the report describes weak density differences between CO_2–saturated and unsaturated brines, and formation heterogeneity as two factors that could hinder this process.

Estimation of Model Boundary Conditions

As outlined above, assignment of realistic boundary conditions is required to establish meaningful predictive models of storage performance and this aspect assumes critical significance where compartmentalisation of DSF is likely, by lateral flow boundaries such as faults or stratigraphic ‘pinch-out’.

Shale permeability estimated by various previous studies of CO_2 storage, petroleum systems analysis and North Sea hydrocarbon field observations is summarised in Table 2 below.

From the data presented in Table 2, the report infers that shale permeability of E-18 m^2 (microdarcy) would yield a relatively high flux boundary condition, whereas E-21 m^2 (nanodarcy) would give a very low flow boundary condition.

Table 2: Literature Review Shale Permeability

Source	*Study area and approach*	*Permeability (m^2)*	*Pth, Hg-air (MPa)*	*Interpretation/Observation*
Zhou *et al.* (2008)	Illinois Basin, numerical	E-17 to E-19	2 to 15	Storage, dynamic capacity
Thibeau & Mucha (2009)	Generic, analytical	E-18	5	Storage, dynamic capacity
Holloway *et al.* (2009)	Bunter Fmn, numerical	E-19	15	Storage, dynamic capacity
van der Meer (2006)	Generic, numerical	'0' ~ E-20 to E-22*	35 to 200 ~ '∞'	No storage, injectivity loss
Economides (2010)	Generic, analytical	'0' ~ E-20 to E-22*	35 to 200 ~ '∞'	No storage, injectivity loss
Corbet & Bethke (1992)	Western Canada, numerical	E-21	85	Regional hydrodynamics
Deming (1994)	Overpressure, analytical	E-21 to E-22	85 to 210	Regional hydrodynamics
Bredehoeft *et al.* (1994)	Uinta Basin, numerical	E-18 to E-20	5 to 35	Cross-formational flow
He and Corrigan (1995)	Overpressure, analytical	E-19 to E-21	15 to 85	Open hydrocarbon systems
Swarbrick *et al.* (2000)	North Sea, numerical	E-21	85	Disequilibrium overpressure
Nordgård Bolås (2000)	North Sea, empirical	E-18 to E-19	5 to 15	Regional trap observations
Bunney & Cawley (2000)	North Sea, empirical	E-19	15	Field observation, Forties

The report considers the empirical relationships that link a series of factors – threshold pressure, depth, porosity and permeability – which govern potential flow through shales. Shale permeability is estimated by two methods:

1. Empirical relationships of porosity-depth-permeability derived from laboratory testing of core samples, and;
2. Observational evidence from North Sea hydrocarbon fields, which derive permeability estimates from the empirical relationship between column heights, shale threshold pressures and shale permeability.

Recent work by Yang and Aplin (2009) has established a transform function for shale porosity and permeability according to clay fraction, based on laboratory test data. For a typical clay fraction range, shale permeability of E-18 m^2 for example, requires porosity in the range 30% to 55%. That permeability range would generally occur at depths too shallow for storage of CO_2 as a supercritical fluid, according to most datasets that link shale porosity to depth.

However, consideration of threshold pressures derived from North Sea regional observations allows a separate calibration which suggests shale permeability in the microdarcy range is likely at depths relevant to large scale storage (Figure 1). This upscaling effect – increasing shale permeability by around two orders of magnitude when moving from core sample to field scales – is a well established phenomenon, due to features such as fractures, faults and gas chimneys being disproportionally absent from core samples. It is analogous to experience in shallow hydrogeological investigations, where laboratory and small-scale field tests typically give values for hydraulic conductivity (a function of permeability) orders of magnitude less than field scale observations ('bulk' hydraulic conductivity or permeability).

Figure 1: Upscaling of Regional Shale Permeability

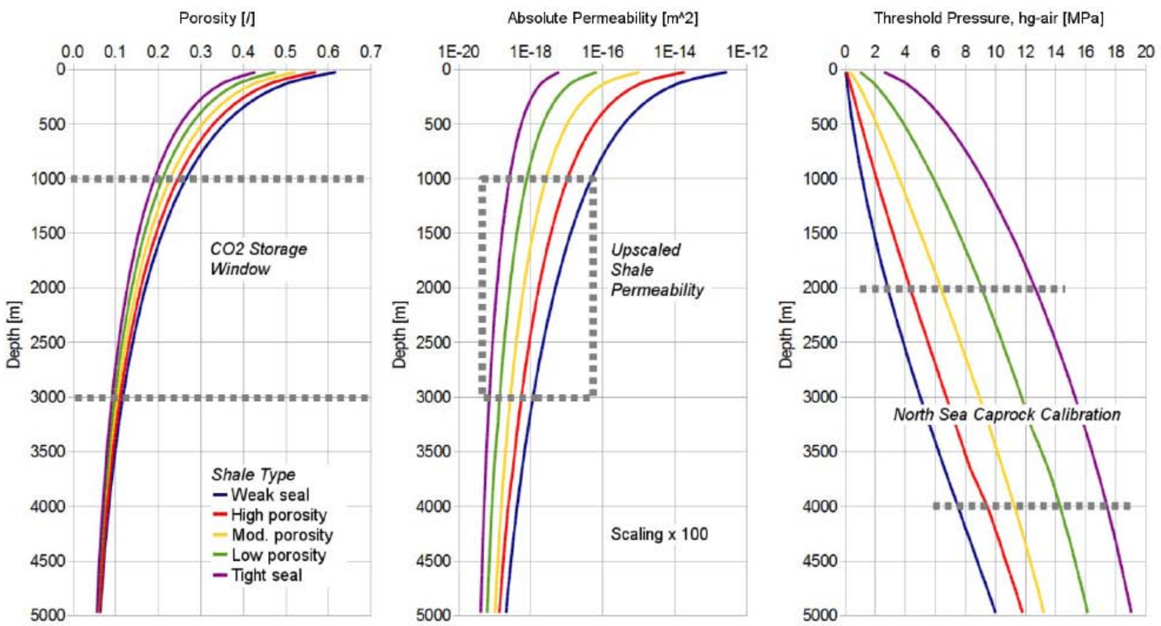

Modelling Scenarios

The study performed a series of modelling exercises to further investigate the effects of boundary conditions on storage performance, considering both analytical and numerical approaches. Analytical models consist of equation(s) that allow first approximations of system behaviour, through use of simplifying assumptions. Numerical models can provide greater accuracy in the assessment of complex systems, but require more comprehensive data input to generate results.

The first modelling exercise comprised an assessment of trapping potential in a large formation, to determine sensitivity to changes in assumed caprock threshold pressures (and therefore shale permeability). The conceptual model comprised a regional storage formation in an area 3,000km^2, with storage depth range from 1,500m to 2,000m; 3 assessments of storage capacity were undertaken for assumed caprock permeability values of E-17 m^2, E-18 m^2 and E-19 m^2, representing weak, moderate and strong seals, respectively. The strong seal with corresponding high threshold pressure, resulted in a plume footprint hundred's of square kilometres, whereas the weak seal resulted in a plume of less than 10 square kilometres.

The study next considered an analytical approach to regional pressurisation. The application of Darcy's Law to this topic can be justified as regional brine displacement is likely to be a single-phase flow phenomenon, in hydrostatic or near-hydrostatic conditions and from storage formations that have much greater lateral extent than vertical thickness. A simple worked example of an analytical solution for a 1Mt/annum 'closed system' (i.e. compartmentalised) storage site showed that caprock permeability of E-18 m^2 would allow brine dissipation to equal the injection rate, thus avoiding pressurisation.

The study then extended this analysis of regional pressurisation by considering sensitivity to changes in caprock permeability and thickness, in the context of various sizes of storage compartment. The following conclusions were drawn:

1. Pressure footprint size is highly sensitive to caprock permeability and thickness;
2. Threshold pressures and CO_2 containment potential are insensitive to caprock thickness;
3. Pressure responses to injection are strongly affected by compartment size and related boundary surface area;
4. An ideal storage scenario appears to be a relatively thin shale caprock with microdarcy permeability – allowing brine dissipation to maintain injectivity while retaining adequate CO_2 containment potential. This permeability is likely to occur in a specific depth window, subject to factors such as shale clay content and burial history;
5. Characterisation of regional shale permeability will be subject to a high degree of uncertainty.

The study proceeded to a case study model, to examine the contributions of solubility and compressibility to storage performance, and to further examine shale permeability effects on pressurisation. This exercise demonstrated that for a total injection of approximately 200Mt CO_2 into a 25m thick sandstone storage formation, of permeability 300mD and at 1,500m depth, within a structural trap of 180km^2 areal extent:

- Over 95% of the storage capacity is dependent on boundary conditions (shale surface area, permeability and thickness) allowing sufficient migration of brine to maintain injectivity;
- Solubility and compressibility effects were collectively only able to provide less than 10% of the required storage capacity;
- Closed system, zero-flux assumptions of boundary conditions would only be appropriate for small compartments bounded by thick shales with nanodarcy-range permeability.

In the final modelling effort performed by the study, a numerical simulation of regional pressurisation was run to confirm findings from the analytical approaches. Modelling was undertaken first for a uniform sandstone storage formation, and then with heterogeneity added based on an SPE standard dataset; results confirmed the findings of the analytical modelling described above. Note also that whilst formation heterogeneity had limited influence on pressurisation, which averaged 5MPa across the storage formation and returned to natural equilibrium within decades, CO_2 migration picked out high permeability channels. This finding has an important implication for pressure relief via brine abstraction wells – as proposed for example in the Gorgon project in Western Australia – in that the location of such wells will need careful design to minimise the possibility of CO_2 breakthrough.

Percolation of brine through the boundary shales was calculated as in the order of millimetres per year – allowing displacement of an equivalent volume of brine to CO_2 into stratigraphic units above and below the storage formation and effectively preventing excessive pressurisation. In real geological settings, natural heterogeneity will result in localised variations in percolation rates and brine fluxes through the shales. The report notes the limited significance of individual faults, fractures and wellbores in controlling overall percolation and flux but reminds the reader that these features could be important in terms of providing direct leakage pathways to shallow potable aquifers. A very simple estimation applied to a hypothetical leaky fault showed a potential brine flux rate of 66,000 kT/year.

Expert Review Comments

Expert comments were received from 7 reviewers, representing industry (corporate sponsors of IEAGHG) and academia. The overall response was positive and highlighted a significant contribution to this area of storage research.

Key technical suggestions made by reviewers related to the modelling work performed during the study; reviewers requested further details on the simulation methodology employed, and also some comment concerning brine flux rates and pressure evolution over time. These comments were addressed in the final report.

Conclusions

Many regional surveys of storage potential around the world have shown DSF to provide the largest theoretical capacity. However, the limited operational experience of large scale injection into DSF and general lack of characterisation data, means a greater level of uncertainty exists in comparison to storage prospects in depleted hydrocarbon fields. A key area of uncertainty relates to the effects of pressurisation on DSF storage performance.

A critical factor in modelling of DSF storage and associated pressurisation effects is the assignment of boundary conditions. Open systems assume formation brine is free to migrate laterally within the storage formation, allowing dissipation of pressure so that injectivity can be maintained. Closed systems assume impermeable boundary conditions to the storage formation, effectively limiting storage capacity to compressibility of rock and pore fluids and creating the likelihood of decreasing injectivity. In this context, the report also noted that dissolution of CO_2 in formation brine may be insufficient to counter the negative effects of a closed system.

Shale is likely to form the predominant vertical boundary layer for most DSF. Given the potential compartmentalisation of many DSF due to such features as sealing faults or stratigraphic thinning (‘pinch out’), the permeability of shale is likely to govern boundary conditions for many storage sites. However, characterisation of regional shale permeability is problematic.

This study, through literature review and modelling exercises, has demonstrated that shale permeability in the order of microdarcies (E-18 m^2) would allow brine migration and therefore alleviation of pressurisation in typical large scale DSF storage projects. In contrast, relatively impermeable shale (E-21 m^2 or nanodarcies) would prevent significant brine migration and lead to loss of injectivity. The report considered empirical relationships between such factors as depth, capillary entry pressure, porosity and permeability; whilst data derived from core scale laboratory analyses suggested that shale could be relatively impermeable at depths relevant to storage, consideration of field evidence from North Sea hydrocarbon fields indicated that regional shale permeability may sufficient to allow brine displacement. This contradiction can be easily explained by up-scaling effects, because laboratory testing of cores biases permeability measurements towards rock matrix, rather than bulk, properties.

Some further key conclusions drawn from the study were as follows:

- Pressure footprint size is highly sensitive to caprock permeability and thickness;
- Threshold pressures and CO_2 containment potential are insensitive to caprock thickness;
- Pressure responses to injection are strongly affected by storage compartment size and related boundary surface area;
- An ideal storage scenario appears to be a relatively thin shale caprock with microdarcy permeability – with brine dissipation maintaining injectivity but with adequate CO_2 containment potential. This permeability is likely to occur in a specific depth window, subject to factors such as shale clay content and burial history;
- Characterisation of regional shale permeability will be subject to a high degree of uncertainty;
- Compressibility of storage formation rock and pore fluids, and dissolution of CO_2 in brine, are unlikely to make major contributions to the alleviation of pressurisation;
- The use of abstraction wells to relieve pressure will require careful design to minimise the likelihood of CO_2 breakthrough, since formation heterogeneity may lead to channelised plume development;
- The closed system approach to modelling DSF storage is only likely to be valid for relatively small pressure compartments and where boundary shale exhibits permeability in the nanodarcy range;

The report is based on literature review and theoretical modelling; further large scale demonstration projects are required to calibrate predictive models and improve understanding of DSF performance.

Recommendations

The issues of pressurisation and brine displacement are likely to remain of great significance to storage potential in DSF, and IEAGHG should ensure that adequate attention is paid to these topics through future storage network meetings and by the study programme.

A future review of the topic would be particularly useful as data is generated by future large scale demonstration projects.

IEAGHG REPORT

Pressurization and Brine Displacement Issues for Deep Saline Formation CO_2 Storage

Andrew Cavanagh, PhD

The Permedia Research Group

Table of Contents

Figures

Tables

Appendix

References

Executive Summary

Worldwide, deep saline formations are expected to store gigatonnes of CO_2 over the coming decades, making a significant contribution to greenhouse gas mitigation. At present, our experience of deep saline formation storage is limited to a small number of demonstration projects that have successfully injected megatonnes of captured CO_2. However, concerns have been raised over pressurization, and related brine displacement within and around deep saline formations, given the anticipated scale of future storage operations. This report aims to address these concerns and their origins in computational and analytical flow models. The report does not address the related impact of brine displacement on shallow potable groundwater, which is the subject of a separate IEAGHG study, to follow in 2011.

Whilst industrial-scale demonstration projects such as Sleipner and In Salah have not experienced pressurization problems, generic flow models have indicated that, in some cases, pressure may be an issue. The problem of modeling deep saline formation pressurization has been approached in a number of different ways by researchers, with published analytical and numerical solutions showing a wide range of outcomes. The divergence of simulation results (either supporting or negating the pressurization issue) principally reflects the *a priori* choice of boundary conditions.

Published modeling approaches can be summed up as either 'open' or 'closed': a) open system models allow the formation pressure to dissipate laterally, resulting in reasonable storage scenarios; b) closed system models suggest pressure changes that may result in a loss of injectivity, caprock leakage and well interference within the storage site, and with neighboring operations. As a consequence, the closed system scenario predicts that storage sites will commonly fail to accommodate the injected CO_2 at a rate sufficient to handle routine projects.

New models, built for this study, aim to demonstrate that closed system approximations of formation pressurization and brine displacement need to be approached at a regional scale and with geologically realistic boundary conditions. Deep saline storage formations are unlikely to have zero-flow boundaries (closed system assumption), and so the pressure relief contribution from the low permeability shales that typically surround storage formations needs to be addressed in such models.

At a field scale, shales are effectively perfect seals with respect to multiphase flow, but are open with respect to single phase flow, and so allow for pressure dissipation via brine displacement at a regional scale. This is sometimes characterized as a 'semi-closed' system. It follows that the rate at which pressure can be dissipated (and CO_2 injected) is highly sensitive to the shale permeability. A common range from approximately millidarcy (10^{-15} m^2) to nanodarcy (10^{-21} m^2) is considered, and the empirical relationships of shale permeability with respect to porosity and threshold pressure are reviewed in light of the regional scale of CO_2 storage in deep saline formations. Our model indicates that, while nanodarcy shales (10^{-21} m^2) will result in significant pressurization, shales in the microdarcy range (10^{-18} m^2) are likely to provide sufficient dissipation via brine displacement to allow for routine geological storage. There is regional evidence, from the North Sea, that typical shale permeabilities at depths associated with CO_2 storage (1-3 km) are likely to favor storage, relegating pressurization to a manageable issue.

In summary, recent concerns regarding pressurization appear to be largely model driven. The scarcity of pressure data for megatonne storage projects has meant that pressure prediction models have been hypothetical in nature. Chief amongst the hypothetical constraints have been assumptions concerning the likely boundary conditions of deep saline formations. In the absence of sufficient calibration data (which will presumably emerge over the coming decade), modeling is at best a sensitivity analysis. As such, the ‘no-flow’ assumption for shales is a poor approximation. The analysis presented here suggests that the flow contribution of shale boundaries to pressure dissipation via brine displacement is significant with respect to CO_2 storage, in accord with long established principles for basin-scale flow dynamics in both the fields of regional hydrology and petroleum systems analysis. The model results suggest that, while pressurization may remain an issue for small restricted storage compartments, future storage operations in regional deep saline formations are unlikely to encounter significant pressurization issues.

1. Background to Geological CO_2 Storage Models

This introduction covers the historical background of CO_2 storage models, from the very early climate research of Guy Stewart Callendar (1938), a steam engineer with an amateur interest in atmospheric observations, to the emergence of the earliest geological storage models by van Engelenburg and Blok (1991), two Dutch scientists with a cultural understanding of gas storage in the Netherlands (where the North Sea natural gas supply is buffered by geological containment). Van Engelenburg and Blok foresaw much of the technical debate surrounding pressurization.

1.1 A Technical Challenge

Recent scientific meetings (e.g. GHGT9, Washington 2008; AAPG Hedberg, Vancouver 2009) have highlighted the need for a better understanding of pressurization and brine displacement models for deep saline formations. This aspect of Carbon Capture and Storage (CCS) has been identified in a recent *Science* review paper as a significant technical challenge (Haszeldine, 2009) with estimates of saline storage capacity being down-scaled by orders of magnitude by some researchers in anticipation of a closed system pressure response. The review paper notes that, given the current state of model uncertainty, the true capacity of saline formations ('niche or major mitigation') will only emerge from observing industrial-scale demonstration projects over the next decade. Published models have returned a wide spectrum of outcomes that range from abundant capacity to none at all. Anticipated capacity estimates help to inform the expectations of researchers and non-technical parties, and test the validity of different conceptual models on the unobserved but relevant timescale of decades to millennia. The calibration of models to studies will also improve the criteria for modeling future storage sites and contribute to site selection criteria.

At present, the technical challenge of pressurization and brine displacement is largely driven by model uncertainty. Some modelers advocate that storage capacity will be severely impacted by injectivity problems, while others suggest much more moderate outcomes. The modeling approaches that result in these contradictory findings are discussed in detail in the following sections; however, the key differences can be summarized as boundary condition assumptions (Table 1). While end-member scenarios with purely open or closed boundary approximations lend themselves to simple reservoir engineering heuristics and resolvable analytical modeling problems, the outcomes are often misleading with respect to the true pressure response of geological CO_2 storage. A conceptual model needs to reflect the storage setting, related flow properties and the boundary conditions associated with storage formations. While natural systems are populated with storage formations that have permeable boundaries, this understanding has proven difficult to abstract for analytical approaches that are an accurate reflection of storage systems.

This report begins with a short overview of the historical background to recent storage models. The background is intended to help place recently published models in their disciplinary context and so contribute to a better understanding of how pressurization and brine displacement issues are conceptualized. The sections that follow critique the assumptions and caveats of these models and summarize the key elements of recent popular approaches to predicting the storage formation pressure response. The report presents a reconsideration of the parameters and assumptions necessary to build and refine CO_2 injectivity models for regional systems that are potentially neither open nor closed. This prepares the ground for the sections that present new analytical and numerical models of injectivity. The aim of these models is to address the significance of permeable boundary conditions and heterogeneous system descriptions for geological CO_2 storage with respect to the pressure response within, and in proximity to, deep saline formations. The models are not intended to address the potential impact of storage on shallow potable water resources, which is beyond the scope of this study.

With respect to permeability units, CO_2 storage modeling is part of an emerging discipline that draws heavily on reservoir engineering, petroleum systems analysis and hydrology. While these share the common ground of Darcy's law and the concept of permeability, the different fields follow different conventions when reporting values. As a result, permeability within this report is expressed in both SI and non-SI units - e.g. one millidarcy may be reported as 1 mD, 10^{-15} m^2, or E-15 m^2 (a more accurate value for the millidarcy is 9.87×10^{-16} m^2, although the integer approximation usually suffices – Appendix A.3). All other measurements follow standard SI notation.

System boundaries	*Brine flux and pressure response*	*Recently published examples*
Open system	*Regional lateral flux; transient local pressurization.*	*Doughty & Preuss, 2004; USDOE, 2008; Nicot, 2008; Chadwick et al., 2009.*
Semi-closed system	*Flux at boundaries; moderate regional pressurization.*	*Zhou et al., 2008; Thibeau & Mucha, 2009; Holloway et al., 2009.*
Closed-system	*Flux limited to storage formation; rapid loss of injectivity.*	*van der Meer & van Wees, 2006; Ehlig-Economides & Economides, 2010.*

TABLE 1: An overview of system boundary conditions. The system boundary classification (after Zhou *et al*., 2008) is divided between the end-member scenarios of open and closed systems, and a pragmatic semi-closed system. Note that analytical models of open systems typically close the vertical boundaries to flow in order to meet the criteria of the equations used to model the system.

1.2 Historical Context

Guy Stewart Callendar, an amateur meteorologist, published *The Artificial Production of Carbon Dioxide and Its Influence on Temperature* in 1938, inferring a significant CO_2-related global temperature increase based on forty years of global weather data and observations (Callendar, 1938). The Callendar paper was the first to hypothesize a link between fossil fuel emissions and climate change, building upon the theory of greenhouse gases proposed by Svante Arrhenius (1859-1927). The idea became known as the 'Callendar effect', i.e. anthropogenic climatic change caused by increases in atmospheric carbon dioxide, primarily from fossil fuel combustion. Observations from the Mauna Loa observatory, Hawaii and Antarctic stations (1958-1969) confirmed the global rise in CO_2 levels (Keeling, 1978) with much scientific debate over cause and feedback mechanisms. Inferred outcomes varied from catastrophic cooling as a result of increased cloud cover (e.g. Budyko, 1969) to catastrophic warming as a result of the greenhouse effect (e.g. Sawyer, 1972). However, both catastrophe positions advocated for carbon dioxide sinks to artificially stabilize the climate, with ocean sequestration being a favoured early candidate (Rasool and Schneider, 1971).

The late 20th Century saw a global political response to atmospheric pollution. Notably in 1987, the *Montreal Protocol* initiated action on ozone depletion, and the United Nations raised the profile of sustainable development with *Our Common Future*, aka the *Brundtland Report* (in recognition of the role played by the Norwegian politician, Gro Harlem Brundtland). *Our Common Future* led to the first *United Nations Framework Convention on Climate Change* in 1992, widely known as the *Rio Earth Summit*, which laid the groundwork for the *Kyoto Protocol* in 1997. The 1990s also saw the publication of the earliest *International Panel on Climate Change* reports, which placed CCS in context as one of a portfolio of climate mitigation strategies. The role of CCS in technology forecasts has increased over the last decade (e.g. Pacala and Socolow, 2004), with the recent IPCC (2005) special report on *Carbon Dioxide Capture and Storage* emphasising the significant storage potential of deep saline formations. The credibility of deep saline formation storage owes much to the notable early success of the Sleipner project (1995 onwards), the first of the megatonne storage sites. Pressure, with respect to deep saline formation storage, has only emerged as a cause for concern within the last decade, although the analytical approaches for flow-related pressure fields are based on models that date back to the late European Enlightenment (Appendix A.1).

1.3 Megatonne Storage Sites

The Sleipner project was planned and implemented in the mid-1990s (Figure 1). Sleipner is a European storage site that injects one million tonnes of CO_2 per year as result of Norwegian tax legislation and Statoil's environmental policies for developing a natural gas field with a high CO_2 content. Sustainable development carbon taxes were pioneered in Scandinavia: Finland introduced legislation in 1990, closely followed by Sweden and Norway in 1991. The Norwegian carbon tax, introduced by Brundtland during her third term as Norwegian Prime Minister, is about $50 per tonne of carbon emissions, and led to the regulation of offshore CO_2 emissions from the petroleum industry. Since 1996, Statoil has captured and stored approximately one million tonnes of CO_2 per year from the production stream of the Sleipner gas field. The Sleipner project was the first example of geological CO_2 storage in a deep saline formation.

The storage formation, Utsira, is extremely large, and is typically treated as an open system. The IEAGHG Weyburn-Midale project, Saskatchewan, Canada, began in the year 2000 and is on a similar scale (17 Mt stored over the first decade) but differs from Sleipner in that the CO_2 is injected into a producing oil field that is actively pressure managed. There is currently one other megatonne storage site in a deep saline formation: In Salah, Algeria, (approximately 3 Mt stored since 2004). Sleipner remains the largest of the three, but will soon be eclipsed by the Australian Gorgon project (expected injection rate of 2 to 4 Mt/yr, commencing in 2014). Both Sleipner and Gorgon must inevitably be dwarfed by the scale of projects required to store gigatonnes of CO_2 within a decade (Haszeldine, 2009). Commonly anticipated injection rates are anticipated to be five-to-ten million tonnes per year per site. The megatonne rate of injection and gigatonne scale of CO_2 storage has led to theoretical concerns regarding the capacity and injectivity of deep saline formations. Models of pressurization have to address these unprecedented scales, and have challenged the modeling community with respect to conceptual models, approach and resolution (Figure 1).

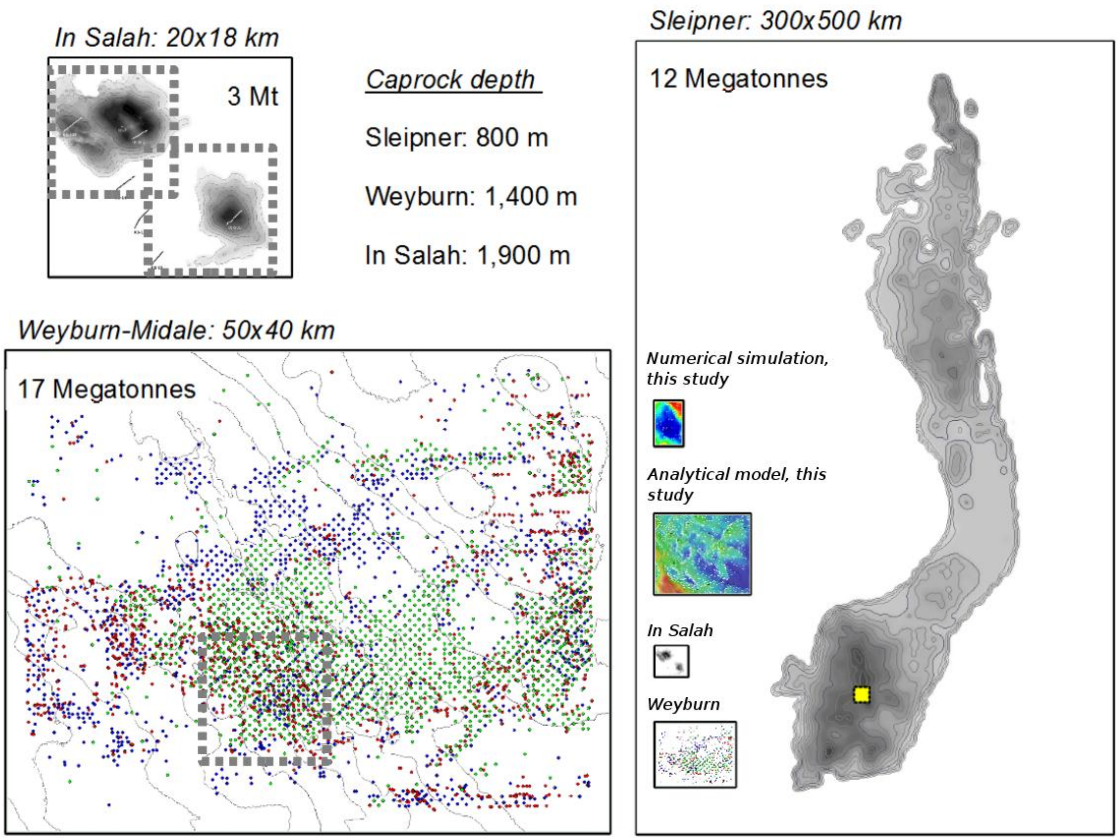

FIGURE 1: Megatonne storage sites. Emission reduction strategies have led to the unprecedented storage of CO_2 in geological formations. All three sites are heterogeneous (fractured and faulted with respect to In Salah and Weyburn; densely populated with wells for Weyburn; and vertically stratified into reservoir units and shale baffles for Sleipner). The dashed gray boxes and yellow square are 10x10 km footprints within which current megatonne CO_2 plumes are found. Pressurization footprints for closed systems are expected to be much larger: for a comparison of scale, the Sleipner regional map also includes the area-of-interest maps for the two other existing megatonne sites and the model extents for the analytical and numerical scenarios used in this study. Pressurization models typically cover an area of hundred-to-thousands of square kilometers.

2. Early Research Models

The Netherlands was the first research community to publish peer-reviewed modeling papers on deep saline formations and CO_2 storage during the early 1990s. The Netherlands has a culture of gas storage dating back to the 1960s, as geological trap structures buffer the natural gas fuel supply from the Southern Gas Basin of the North Sea. The University of Utrecht and TNO National Geological Survey undertook preliminary appraisals that attempted to match potential capture projects to storage sites, with the earliest study by van Engelenburg and Blok (1991) touching on injectivity. Another study by van der Meer (1992) attempted to estimate the regional capacity for the Netherlands, although this was an early geometric approach, with pressurization and injectivity considerations only featuring in his much later work (van der Meer and van Wees, 2006). Other regional studies followed, notably from North America with its longstanding culture of CO_2 injection for enhanced oil recovery. The first Albertan estimate (Bachu *et al.*, 1994) and USA estimate (Bergman and Winter, 1995) took similar approaches to the early Dutch research.

2.1 Pressurization and Injectivity

A study at the University of Utrecht (van Engelenburg and Blok, 1991) undertook a financial and technical feasibility appraisal of the Netherlands in the early 1990s that anticipated many aspects of the current debate regarding deep saline formations. The 1991 report and subsequent peer-reviewed paper (van Engelenburg and Blok, 1993) made a number of lucid comments on the technical aspects of injectivity with respect to compressibility, solubility and boundary flow that anticipate the adaptation of reservoir engineering heuristics from natural gas storage to CO_2 storage. The study also highlights the uncertainties inherent in capacity estimates at both the site and regional scale, questioning the validity of quantitative generalizations given the typically poor data control and the site-specific nature of variables. The key technical points of the paper concern solubility, pressurization and formation water displacement. These are summarized and commented on below.

2.2 Open System Injectivity

The injectivity of a laterally open system can be estimated using a simple rule-of-thumb, or heuristic and analytical approaches based on Darcy's law. As a first approximation, van Engelenburg and Blok (1993) adapt a flow rate equation normally used to calculate natural gas production from wells (Appendix A.4). The paper clearly states a number of assumptions associated with this approach:

- The formation has closed vertical boundaries (two-dimensional abstraction).
- The formation is horizontally infinite (laterally open boundaries).
- The ambient pressure of the reservoir remains at hydrostatic conditions (open system response).
- The formation is homogeneous and isotropic (radial flow and uniform sweep).

All four assumptions are common approximations when abstracting hydrocarbon field production to a single-well single-phase flow model. This approach can also be found in numerous recent analytical models of CO_2 storage (e.g. Nicot, 2008; Oruganti and Bryant, 2010). The first three conditions reduce the system to a two-dimensional problem suitable for the adaptation of the reservoir engineering heuristic. The fourth condition implies a symmetrical flow or sweep of gas away from the well. The paper does not explicitly state the problematic assumption of single-phase flow given the two-phase flow nature of CO_2 storage, and also assumes sub-critical pipeline conditions for CO_2 at 6 MPa and 15ºC.

Van Engelenburg and Blok report that for likely input ranges the possible flow rate for CO_2 injection around one third-to-one megatonne per year per well. This is surprisingly low given the ideal open system approach. The low estimate results from a conservative pressure limit for injection at only 109 percent of the initial reservoir pressure. Later proponents of closed systems (e.g. van der Meer and van Wees, 2006; Ehlig-Economides and Economides 2010) have criticized the open system approach as unrealistic. However, van Engelenburg and Blok (1993) are clearly aware of the method's limitations, stating that the abstraction is only intended as a first-order approximation. The paper states that actual flow rates are likely to be less than the high-end open system estimate and goes on to consider the injectivity of a closed system, stating that the formation pressure may be expected to increase substantially. The paper points out that compressibility, solubility and brine displacement are the three principle mechanisms that may compensate for the injection-induced pressurization in a system that approximates to having closed boundaries.

2.3 Closed System Compressibility

Van Engelenburg and Blok assume that porewater provides the principle compression response in a closed system. For a water compressibility of around 5E-10/Pa, equivalent to a 0.05 percent porewater volume change for a megapascal increase in pressure (Figure 2), the porewater compression response amounts to a fraction of a percent for the megapascal changes in pressure expected with CO_2 injection. The paper observed that porewater compression would fail to prevent significant pressurization. This approach (a closed boundary and low compressibility estimate) is the crux of all the poor injectivity models that have emerged over the last two decades. Indeed, recent closed system compression-dominated analyzes by van der Meer and Economides have added very little to the substance of the early work by Van Engelenburg and Blok, who noted that a perfectly closed system is geologically unrealistic with respect to seal permeability and formation water displacement. However, both these early and later analyzes underestimate the contribution of rock compression.

Deep saline formation rocks have a similar compressibility to porewater at around E-09 to E-10/Pa (Mucha and Thibeau, 2009). The rock compression response to pressure is typically much larger than the porewater contribution as the rock-to-brine volume ratio is around 3:1. Recent numerical simulations that apply a 'pressure cell' approach (e.g. Heinemann *et al.*, 2010) have reappraised the contribution of compressibility to the potential storage of CO_2 in large formations. The Heinemann simulation for the Bunter Formation, a regionally extensive deep saline formation in the southern North Sea, UK, estimates a resource potential in the gigatonne range assuming compression alone in a large closed system. As an appraisal of the contribution to storage within a small pressure compartment (15x25 km), described below in the section on analytical models, suggests that the commonly held assumption concerning the slight contribution of compressibility to storage is only valid for storage in very small compartmentalized formations. For moderate compartments (i.e. hundreds of square kilometers) the contribution may be significant with respect to short term storage (tens of megatonnes) and planning (water abstraction strategies).

Recent work by Thibeau and Mucha (2009) also suggests that for a closed system response, the compression of a moderately sized deep saline formation would provide sufficient time (i.e. years-to-decades) to either engineer a solution to low injectivity, such as pressure relief wells and water abstraction, or find relief storage elsewhere before the injectivity of the site failed. However, a compressibility-dominated scenario is a conservative approximation given the potential for the natural dissipation of pressure via porewater migration at the boundaries of a storage formation.

2.4 Plume Solubility

Solubility is tentatively addressed by van Engelenburg and Blok (1993), indicating the early state of knowledge with respect to this aspect of storage. Their approach reasonably assumes that, as a first approximation, the water available for saturation is equivalent to the irreducible porewater fraction of the formation exposed to CO_2. This approach remains a credible assumption (e.g. Thibeau and Mucha, 2009). Van Engelenburg and Blok estimate a 1.4% contribution for dissolved CO_2 as a fraction of the mass injected. Thibeau and Mucha (2009) estimate around 2%. Both studies assume a CO_2 solubility of 50 kg/m^3 of porewater. Solubility increases with respect to pressure, but decreases with respect to temperature and salinity. While the 50 kg/m^3 approximation is accurate for freshwater at surface conditions, recent papers on plume dissolution (Hassanzadeh *et al.*, 2008; Spycher *et al.*, 2005) indicate that CO_2 solubility drops to around 20-40 kg/m^3 for storage conditions.

Both studies also assume low levels of irreducible porewater at around 15-20%. Recent work by Luo *et al.* (2008) favors a wider range at 20-40% (Table 2). The contribution of CO_2 dissolution to storage on injection-and-monitoring timescales remains uncertain. It appears likely that the porewater associated directly with the plume (i.e. the brine within pores within the plume) will only contribute a few percent of the storage required (Table 2). It follows that solubility will have little impact on pressure unless a considerable additional amount of CO_2 dissolves into the surrounding storage formation during the injection phase. Diffusion is widely acknowledged to be too slow a process to make a difference on injection timescales. The contribution of density-driven convection is difficult to ascertain but thought to be modest given formation heterogeneity and the weak density difference for saturated and unsaturated brines (e.g. Bjørlykke, 1994; Rapaka *et al.*, 2008).

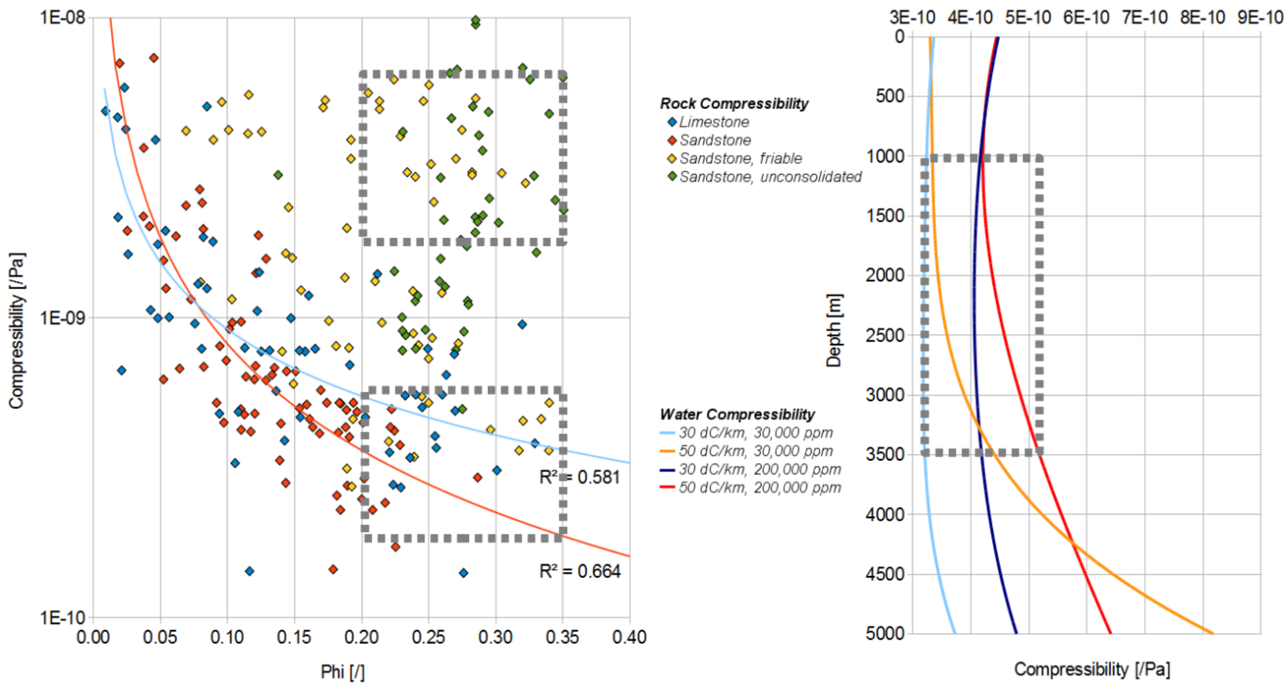

FIGURE 2: Rock and water compressibility. Rock compression depends on the strength of the rock matrix (Newman, 1973). Unconsolidated and friable material is more compressible by about an order of magnitude for typical storage formation porosities. Cemented sandstones have a compressibility of approximately 2E-10 to 6E-10/Pa over the same range. Limestones have a similar compressibility. Water is sensitive to pressure, temperature and salinity (Rowe and Chou, 1970). Typical brine compression is approximately 3E-10 to 5E-10/Pa for likely storage formation depths. The gray boxes show the field of values from which first-order approximations have been made: consolidated storage formation: 5E-10/Pa. Unconsolidated: 5E-09/Pa. Water: 4E-10/Pa.

Contribution	*Swc*	*Sgas*	*Ratio*	*Solubility*	*Plume Mass*	*Dissolved Mass*
Low estimate	*0.20*	*0.80*	*1:4*	*20-40 kg/m³*	*98-99%*	*1-2%*
Mid estimate	*0.30*	*0.70*	*3:7*	*20-40 kg/ m³*	*97-98%*	*2-3%*
High estimate	*0.40*	*0.60*	*2:3*	*20-40 kg/m³*	*95-97%*	*3-5%*

TABLE 2: A comparison of the potential solubility contributions to storage for a plume-associated volume of saturated porewater. Low, mid and high estimates are a first approximation for the method outlined in the text, following van Engelenburg and Blok (1993) and Thibeau and Mucha (2009). *Swc*, the irreducible connate water saturation; *Sgas*, the separate phase CO_2 saturation. *Ratio*, the volumetric ratio of water to gas.

2.5 Brine Displacement and Shale Permeability

Van Engelenburg and Blok (1993) noted that deep saline formations are unlikely to be closed systems as they are flanked by low permeability rocks such as shales that have dynamic boundary fluxes for brine. As the study points out, the question then becomes a matter of volumes and rates, requiring an analytical or numerical approach beyond the scope of their study. The necessary empirical relationships for modeling such systems were scarcely available in 1991, but have been published over the last decade (e.g. Sorkhabi and Tsuji, 2005; Yang and Aplin, 2009). The first paper to address such an approach for CO_2 storage is the Illinois Basin study by Zhou *et al.* (2008).

While van Engelenburg and Blok (1993) declined to speculate on pressure dissipation and the displacement of porewater at the boundaries of a storage formation, given the poor data and numerical tools of the time, the study did draw attention to the success of compressed air geological storage experiments and the general evidence for the hydrodynamic nature of the subsurface (e.g. Hubbert, 1953; Tóth, 1963). It has since been argued that such regional hydrodynamics is a function of pressure compensation on geological timescales and that the compressed air storage analogy fails as it is on a much smaller scale than CO_2 storage (van der Meer and van Wees, 2006; van der Meer and Egberts, 2008). The van der Meer analysis is addressed below; however the critical question raised by both sides of the argument is related to shale permeability: *Are typical shale permeabilities high enough to mitigate the pressure response on a regional scale and at expected injection rates?*

The key to testing the contribution of low permeability boundaries to pressure dissipation in deep saline formations, in the absence of the equivocal data that will presumably emerge from large industrial-scale storage projects, is a single-phase Darcy flow analysis. The pressure response within a storage formation and the related brine flux through the surrounding shales will be sensitive to such boundary rock properties as the shale thickness and the shale permeability. Early hydrodynamic regional simulations of groundwater flow induced by pressure changes have been applied to a number of modeling scenarios (Bredehoeft, 1983; Garven, 1989; Deming and Nunn, 1991). However, the timescales of CO_2 storage are very different from natural groundwater flow systems and overpressure in petroleum systems. Such a model would need to establish the flow response of a seal on the injection timescales of months-to-years for reasonable mudrock permeabilities and local megapascal pressure changes. Recently published relationships for permeability and their use in such models are addressed in detail in the sections that follow.

2.6 The Van Der Meer Analysis

In 1992, the Dutch Geological Survey, TNO, estimated that the available storage space for favorable geological formations beneath the Netherlands would be a few percent of the actual pore space due to viscous fingering and gravity segregation (van der Meer, 1992). Van der Meer's early work introduced the concept of a 'storage coefficient' for geological CO_2 storage, also known as an 'efficiency factor', which borrowed from the reservoir engineering concept of recoverable hydrocarbons as a fraction of the hydrocarbons in place. Further studies followed suit, notably from North America, with estimates of the Albertan storage resource potential by Bachu *et al.* (1994) and the USA storage resource potential by Bergman and Winter (1995) employing similar storage coefficients.

An early paper by van der Meer (1995) formalized the concept and methodology of the storage coefficient. Recent studies have since refined the method into a sophisticated and rigorous statistical appraisal method for establishing resource estimates at the regional scale (e.g. CSLF, 2008; IEAGHG, 2009; USDOE 2010). Such reviews have continued to return probable efficiency factors of around two percent (Table 3), supporting the consensus view that there is an abundant global resource for geological CO_2 storage.

However, in the last decade, van der Meer has critiqued the storage coefficient approach as overly optimistic. His critique assumes that deep saline formations will respond to industrial injection rates as a closed system (van der Meer and van Wees, 2006; van der Meer and Egberts, 2008). The van der Meer papers do not test the closed system assumption, as the choice of simulator necessitates a closed system approach. However, the papers do illustrate that, for a regionally confined storage formation with zero flux at the formation boundaries, the pressure response is such that injectivity would be lost within years without pressure management and water abstraction.

Formation	*Possible, P90*	*Probable, P50*	*Possible, P10*
Clastic	*2.0%*	*2.5%*	*6.0%*
Dolomite	*2.5%*	*3.0%*	*5.5%*
Limestone	*1.5%*	*2.0%*	*3.5%*

TABLE 3: Recent storage coefficient estimates by formation types, assuming open boundary conditions (adapted from IEAGHG, 2009). All values rounded up to the nearest half percent. As a first approximation, the regional resource is probably around 2-3% (P50) of the total pore space. The IEAGHG report estimates that a closed system will reduce this estimate by approximately one third to one sixth of the open system estimate, i.e. 0.3-1% (P50).

2.7 Summary of Early Research Models

Early Dutch research pioneered both the estimates of storage resources and the concerns related to boundary conditions and pressure. The resulting dilemma is that the capacity and injectivity of regional storage formations are strongly dependent on the boundary response to pressure changes. Van Engelenburg and Blok (1993) summarized their technical arguments relating to pressurization and brine displacement as follows:

- For a closed system, compressibility and solubility will fail to compensate for pressurization.
- Injectivity will fail unless a significant volume of brine is displaced beyond the formation boundaries.
- The displacement effect is difficult to estimate given simulator limitations and data constraints.

Given that the van Engelenburg and Blok (1993) study was a preliminary evaluation, and the research field was fledgling in nature, the paper is remarkably prescient. The paper concluded that the pressurization issue would be best addressed by modeling. The Dutch Geological Survey, TNO, went on to address simple open and closed system simulations, as published by van der Meer *et al.* (1992, 1995, 2006) that illustrated the significance of boundary flux to pressure in deep saline formations:

- An open system efficiency factor is likely to be around two percent of the available pore space.
- A closed system probably reduces the efficiency to less than one percent. Injectivity becomes critical.

The first CO_2 storage models to assign non-zero permeabilities for shale boundaries have only recently emerged (e.g. Zhou *et al*., 2008; Birkholzer *et al.*, 2009), although precedents for regional hydrology and petroleum system analysis date back to the early 1990s and beyond (e.g. Bredehoeft and Hanshaw, 1968; Neuzil, 1986; Deming, 1994). However, these early models from related disciplines differ in that they address the occurrence of naturally overpressured zones over geological timescales. The injection-induced pressurization that results from the large fluid volumes and short timescales of CO2 storage is a relatively new and challenging problem for modelers, as discussed in the following section on recent analytical models that use closed system approximations.

3. Recently Published Closed System Models

The following section reviews recent analytical approaches to the closed system approximation for CO_2 storage. As different models and interpretations have emerged, most researchers have advocated for a pragmatic interpretation of the closed system model as an end-member approximation with respect to geologically realistic boundary conditions. However, a recent exception is the skeptical analysis by Ehlig-Economides and Economides (2010).

3.1 A Closed System Analysis

A recent closed system analysis by Ehlig-Economides and Economides (2010) is notable for two reasons: 1) the paper briefly received a small amount of international press attention due to its sensationally pessimistic conclusions on the viability of CCS. 2) The findings of the paper have been strongly refuted by the wider scientific community. For example, the *American Petroleum Institute* responded with a published statement that summarized their position:

> "…A number of mis-statements and erroneous base assumptions which could lead readers to arrive at inappropriate conclusions." *American Petroleum Institute*, 15th April, 2010.

A formal reply to the paper, and technical discussion of the flawed assumptions that underlie the analysis, has now been published by the Journal of Petroleum Science and Engineering (Cavanagh *et al.*, 2010). Given the unequivocal statement by the *American Petroleum Institute*, what went wrong? It is clear that the Economides analysis takes advantage of the no-flow boundary approximation to propose an exaggerated and highly unlikely scenario that results in extreme pressurization. Assuming no flow and perfect seals for pressure compartments will always result in an analytical solution dominated by the small contribution of compressibility to pressure dissipation (Figure 3). It is well understood that overly simplistic scientific analogies result in misleading, if mathematically rigorous, proofs such as the apocryphal analysis that bumblebees cannot fly (Peterson, 2004). This invokes the modeling maxim that an accurate framing of a conceptual problem is of vital importance, as models may appear to support a false proposition when founded on a misleading premise and erroneous assumptions.

In the final analysis, both analytical models and numerical simulations need to be compared to real-world data (bumblebees are commonly observed to fly). At present, there is no storage site data to support the Economides analysis. Results from twenty projects globally have recently been reviewed by a Scottish CCS stakeholder (SCCS, 2010). Of these, at the megatonne scale, three major storage projects have been undertaken since 1996: Sleipner, In Salah and Weyburn. None of these have experienced pressurization problems. Globally, there are nine sites that are at an industrial scale, storing 1-to-130 Mt of CO_2 during the project lifetime. Only the Midwest Regional Carbon Sequestration Partnership project at the Burger Plant, Shadyside, Ohio, has experienced severe pressure problems (USDOE, 2009; MRCSP, 2010), with a pressure build-up from 5-to-37 MPa over a few hours. The Shadyside project was canceled in 2008 after a small fraction of the intended 3,000 tonnes CO_2 was injected. This is not surprising as the post-injection analysis showed the formation permeability to be extremely low at around 1-to-10 µD. By contrast, K12-B (20 mD) and In Salah (5 mD) are storage sites with low but adequate permeability, when combined with thickness (i.e. injectivity), and are on schedule to store several millions tonnes of CO_2 at each site.

3.2 Analytical Pressure Models

A number of researchers have addressed realistic scenarios for deep saline formation CO_2 storage (e.g. Muggeridge *et al.*, 2005; Birkholzer *et al.*, 2009). The Muggeridge analysis comprehensively reviews pressure models from the petroleum systems literature of the 1990s that provide analytical solutions for pressure dissipation via Darcy flow out of a pressurized compartment. The paper assumes, *a priori*, that the contribution of flow through low permeability boundary rocks is significant, as this has been a feature of closed system analytical solutions for basin models since the foundational work on regional hydrodynamics by Bredehoeft and Hanshaw (1968). This is the key difference between extreme pressurization models and more moderate solutions (Figure 3).

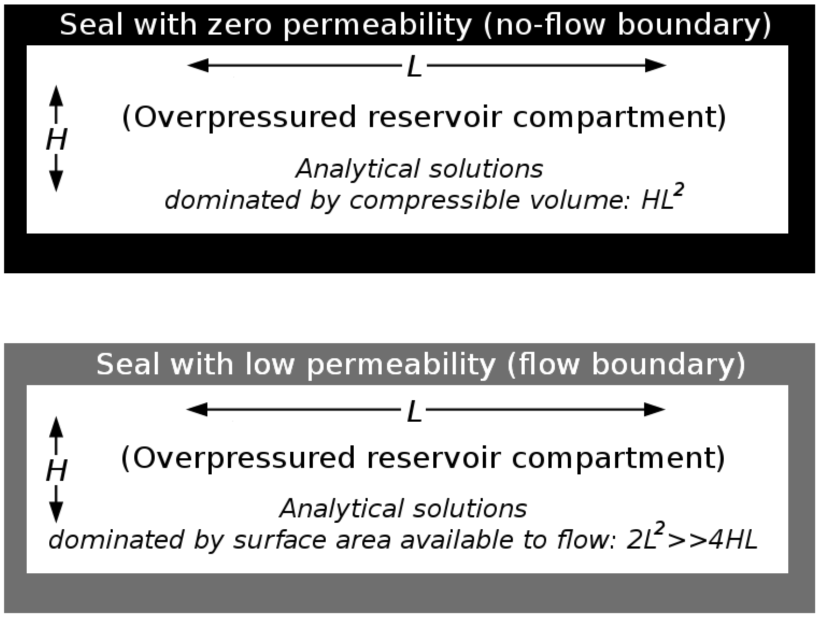

FIGURE 3: Closed system approximations. The black bordered box assumes no-flow boundaries as a result of zero permeability. The analytical solution tends towards extreme pressurization as a result of the dependence on the compartment volume (HL^2) and the related rock and brine compressibility within the storage compartment, which tend to be low at around 5E-10/Pa. The gray bordered box assumes boundary-mediated flow for brine, which is displaced out of the compartment through the surrounding shales. The analytical solution lends itself to a one-dimensional abstraction as the surface area of the upper and lower boundaries is much larger than the surface area associated with the lateral boundaries ($2L^2 >> 4HL$).

Muggeridge *et al.* (2005) also carefully outlines the single-phase, one-dimensional abstractions of common analytical solutions. Firstly, for CO_2 storage compartments, the boundary surface area available to single-phase flow (equivalent to the surface area of the compartment) is much larger than the fraction of the boundary surface area associated with the two-phase plume (single-phase abstraction) as the footprint of a CO_2 plume is much small compared to the related pressure footprint. Secondly, assuming permeable upper and lower shale boundaries, the contribution of the lateral boundaries to a closed system analytical solution is likely to be insignificant (one-dimensional abstraction) as the combined area of the upper and lower surfaces is much larger than the area of the lateral boundaries (Figure 3). For example, the lateral boundary-flux contribution for a small pressure compartment, abstracted to a simple box, with an area of approximately 100 km^2 (10x10 km), and an average thickness of 50 m, is around one percent of the total boundary surface area:

- The surface area for the upper and lower boundaries ($2L^2$): 200,000,000 m^2.
- The surface area for the lateral boundaries (4LH): 2,000,000 m^2.

The Muggeridge analysis concludes that a small pressure compartment (on the scale of a typical hydrocarbon reservoir) will return to normal hydrostatic pressure over tens of thousands of years, if not longer. However, the analysis has a petroleum system focus that principally addresses naturally overpressured compartments with very low seal permeabilities (nanodarcy range, i.e. $<10^{-20}$ m^2), and so does not consider the more significant question for CO_2 storage: *under what conditions will the boundary flux for displaced porewater match the CO_2 injection rate?*

Such a match will result in a dynamic pressure equilibrium within the compartment that allows for CO_2 storage, as long as the maximum pressure does not exceed the limit for site integrity associated with geomechanical failure, fault reactivation and caprock seal integrity (e.g. Rutqvist *et al.*, 2007; IEAGHG, 2010).

Le Gallo (2008) has undertaken a regional modeling study of the Paris Basin with a general approximation for the caprock permeability (reported as "a major regional shale with a very good sealing property"). The simulation results suggest that nanodarcy range permeabilities may have been used, as indicated by the very high levels of pressure perturbation (in excess of 20 MPa close to the injection wells). The pressurization impact extends over long distances (the radius of influence around the injector extends to about 50 km laterally within the storage formation). As a consequence, the paper raises concerns regarding the potential impact of brine displacement on shallow aquifers and the influence of pressure on neighboring CO_2 and hydrocarbon operations. The findings are similar to work by van der Meer *et al.* (2006; 2008). However, the le Gallo study implies that regional nanodarcy shales approach the no-flow boundary approximation, illustrating the need for evidence-based shale permeability characterization.

Papers by Zhou and Birkholzer (e.g. Zhou *et al.*, 2008; Birkholzer *et al.*, 2009) have recently addressed closed system approximations that specifically consider the significance of shale permeability on the likely far-field impact of pressurization and brine displacement. These papers distinguish between perfectly sealed compartments and more realistic 'semi-closed' compartments that are bounded by low permeability shales. Zhou and Birkholzer compare analytical models and numerical solutions using derivations of the Laplace equation (after Tóth, 1963; Bear, 1972). They conclude that permeabilities in the microdarcy range (10^{-17} to 10^{-19} m^2) are likely to result in significant pressure dissipation, allowing for effective injection. Indeed, they consider that shale permeabilities of less than a microdarcy will effectively behave as an open system, potentially resulting in far-field and near-surface pressure perturbations, as investigated by Nicot (2008). They also conclude that shales with permeabilities in the nanodarcy range (10^{-20} to 10^{-22} m^2) will potentially result in a pressurization effect that limits injectivity. With respect to brine displacement, they consider that near-surface impacts are likely to be minimal due to the baffling effect of the layered aquitards and aquifers that are typical of basin stratigraphy. Similar modeling results have also been reported by Yamamoto *et al.* (2009), who demonstrate that shale permeability assumptions are critical to regional-scale pressure models.

3.3 Discussion of Closed System Approximations

From a review of current CO_2 injection and storage experiments, and a comparison of these with long-established models and concepts for hydrocarbon trapping and petroleum systems, it is apparent that subsurface reservoirs are not hermetically sealed, but instead are flanked by low permeability rocks such as shale. The permeability of these shale boundaries at the reservoir top, base and sides is low but crucially not zero. Accurate and appropriate three-dimensional fluid flow models of reservoirs can simulate the feedback effect of the permeability of the enclosing shale rocks on the pressure build-up inside the reservoir during CO_2 injection. Published data, described in the following section, shows that a critical range of values exist for shales that retain oil and gas as a seal. These are within the range of shale permeabilities measured globally by Yang and Aplin (2009) amongst others. However, if the enclosing permeabilities are very low (nanodarcy range), then insufficient fluid transmission occurs and the pressure increases significantly in the reservoir formation. Shales with such low permeabilities appear to be uncommon in the subsurface at the depths envisaged for CO_2 storage, as described in the following section, and are more typically associated with deeply buried zones of naturally elevated pressures. Such reservoirs are not prime candidates for CO_2 storage, and do not feature as abundant storage in global assessments, primarily because of the expense associated with drilling deep deviated wells. Therefore, it is unlikely that CO_2 storage will reflect the extreme cases initially highlighted by van der Meer *et al.* (2006; 2008) and then returned to by Ehlig-Economides and Economides (2010).

3.4 Summary of the Critique

In summary, extreme pressurization scenarios appear to result from overly simplistic closed system approximations, based on unsupported assumptions about subsurface geology and regional fluid flow in the sedimentary basins. More realistic models have appeared in recent publications that examine the full spectrum of closed system approximations. The Economides analysis, when placed in the context peer-reviewed papers, appears to be an extreme end-member approximation that exaggerates the potential significance of pressurization. While pressure remains a potential cause for concern, which needs to be considered when planning a storage site, this technical issue is widely anticipated and well understood. As the following section on empirical evidence shows, the choice of boundary conditions for pressure modeling is paramount and needs to be evidence-based.

4. Empirical Relationships of Trapping and Flow

A much-quoted aphorism, attributed to the statistician George Box, is that "essentially, all models are wrong, but some are useful" (DeGroot, 1987). The value of models frequently lies in their ability to challenge our assumptions concerning fluid flow in permeable rocks. Not surprisingly, CO_2 storage models are bringing to light new challenges in established relationships with respect to porous and permeable media. The evidence for, and appropriate capturing of, general relationships for threshold pressure, permeability, saturation and porosity is the subject of this section, which begins with a comparison of boundary conditions for CO_2 storage models with published values from the similar discipline of petroleum systems analysis. Given the wide range of potential shale permeabilities, the section goes on to describe the empirical relationships used to define the shale permeability, porosity, and threshold pressure. The inter-dependent nature of these empirical relationships is explored, including the significance of regional field-scale observations for scaling transforms and the variable nature of the porosity-depth relationship.

4.1 CO_2 Storage and Petroleum Systems Comparison

The advent of unprecedented megatonne gas injection experiments over the last decade has provided an extraordinary opportunity to test the established relationships for permeability and threshold pressure in the low permeability rocks that define geological flow systems. General assumptions and common relationships for shale threshold pressures and permeabilities in CO_2 storage models can be compared to similar published estimates for petroleum systems (Table 4).

Source	*Study area and approach*	*Permeability (m^2)*	*Pth, Hg-air (MPa)*	*Interpretation/Observation*
Zhou et al. (2008)	*Illinois Basin, numerical*	*E-17 to E-19*	*2 to 15*	*Storage, dynamic capacity*
Thibeau & Mucha (2009)	*Generic, analytical*	*E-18*	*5*	*Storage, dynamic capacity*
Holloway et al. (2009)	*Bunter Fmn, numerical*	*E-19*	*15*	*Storage, dynamic capacity*
van der Meer (2006)	*Generic, numerical*	*'0' ~ E-20 to E-22**	*35 to 200 ~ '∞'*	*No storage, injectivity loss*
Ehlig-Economides (2010)	*Generic, analytical*	*'0' ~ E-20 to E-22**	*35 to 200 ~ '∞'*	*No storage, injectivity loss*
Corbet & Bethke (1992)	*Western Canada, numerical*	*E-21*	*85*	*Regional hydrodynamics*
Deming (1994)	*Overpressure, analytical*	*E-21 to E-22*	*85 to 210*	*Regional hydrodynamics*
Bredehoeft et al. (1994)	*Uinta Basin, numerical*	*E-18 to E-20*	*5 to 35*	*Cross-formational flows*
He and Corrigan (1995)	*Overpressure, analytical*	*E-19 to E-21*	*15 to 85*	*Open hydrocarbon systems*
Swarbrick et al. (2000)	*North Sea, numerical*	*E-21*	*85*	*Disequilibrium overpressure*
Nordgård Bolås (2005)	*North Sea, empirical*	*E-18 to E-19*	*5 to 15*	*Regional trap observations*
Bunney & Cawley (2007)	*North Sea, empirical*	*E-19*	*15*	*Field observation, Forties*

TABLE 4: Shale permeability values from recent modeling studies. The first group is for CO_2 storage. The second group is related to petroleum systems analysis. The third group are observations based on North Sea hydrocarbon fields.*Nanodarcy permeability range (E-21 m^2, equivalent to 10^{-21} m^2, nD) abstracted by the cited authors to a no-flow boundary condition, equivalent to a zero permeability and an infinite threshold pressure.

Recently published CO_2 storage models have assumed various shale permeabilities from effectively zero to upwards of a microdarcy. The related discipline of petroleum systems analysis estimates permeability to be in the micro-nanodarcy range, with a body of work emerging in the nineties on overpressure and hydrocarbon trapping.

A comparison of the two research fields reveals that the zero permeability approximation is only justified as an abstraction for the lowest end of a spectrum that ranges from 10^{-17} to 10^{-22} m^2. A number of general observations can be drawn from the comparison beyond the wide apparent range in variable modulation:

- A no-flow assumption for permeability is much lower than the common range of 10^{-17} to 10^{-22} m^2.
- As a first approximation, a low flux boundary condition would have a nanodarcy permeability, i.e. 10^{-21} m^2.
- As a first approximation, a high flux boundary condition would have a microdarcy permeability, i.e. 10^{-18} m^2.
- The equivalent threshold pressures for the common range are approximately 2 to 200 MPa for mercury-air.
- 2 MPa is equivalent to tens of meters column height for CO_2, i.e. low but acceptable, with good injectivity.
- 200 MPa is equivalent to thousands of meters of column height, i.e. extremely high, but very poor injectivity.
- The North Sea observations were made over a depth range of 2000 to 4000 meters for oil and gas fields.
- The North Sea observations suggest that, for CO_2 storage depths, the range is likely to favor injectivity.
- The North Sea observations can be used to upscale the empirical relationships to a regional approximation.
- Scaling the relationships to field observations matches 10^{-18} m^2 to 2000 meters and 10^{-19} m^2 to 4000 meters.

4.2 The Co-dependence of Empirical Relationships

The permeability-threshold pressure transform and other empirical relationships form a chain of co-dependent parameters for flow in porous media. The threshold pressure-permeability-porosity-depth chain is typically audited with respect to laboratory data; however their application to numerical simulations needs to be validated with field-scale observations, given that micro- to meso-scale laboratory measurements do not necessarily scale to macroscopic field-scale behavior as addressed in regional flow simulations. Each relationship is reviewed in turn below.

4.3 Threshold Pressure-Permeability Power Law

Purcell (1949) originally established the mercury-injection method for estimating absolute permeability from the observed capillary pressure (Appendix A.2). This power-law relationship is a cornerstone of flow models for continuum and conditional approximations of single-phase and multi-phase flow (i.e. groundwater flow as a function of permeability, and gas trapping as a function of threshold pressure). More recently, Sorkhabi and Tsuji (2005) have reviewed the capillary pressure-permeability relationship in detail, concluding that the power-law approximation holds across the common range of clay, silt and sandstone lithologies found within sedimentary basins, and is also applicable to faulted and fractured media. For this study, the available permeability-threshold pressure data has been further reviewed, improving the coefficient of determination from $R^2 = 0.72$ (N =244, Sorkhabi and Tsuji, 2005) to $R^2 = 0.88$ (N=302, this study). The three data sets used for this study also extend the range to nanodarcy permeabilities (Figure 4).

4.4 Permeability-Porosity Transform

Yang and Aplin (2009) have established a transform function for shale porosity and permeability based upon the clay content of shales. The data sets are subdivided by clay fraction with low clay content shales having the highest permeability for a given porosity. The Yang and Aplin transform is generated as a polynomial function derived from curve fitting algorithms, resulting in an improved fit compared to traditional power law representations (Figure 5). Considering the permeability range of interest for CO_2 storage (i.e. micro-to-nanodarcy) it is apparent that any given permeability may occur over a range of porosities depending on clay content. Assuming porosity reduction as a function of depth, it is also apparent that some shales will be weak seals and good pressure dissipators while other shales will be strong seals but poor pressure dissipators. However, without *a priori* knowledge of the caprock shale's clay content and the porosity-depth relationship, a storage formation response can only be estimated as an order-of-magnitude approximation for the likely boundary permeability range. Furthermore, the porosity and permeability data that informs the transform is observed in the laboratory at the microscopic scale. This relationship is likely to be sensitive to scaling and as such requires adjustment to regional field-scale observations such as those documented by Nordgård Bolås *et al.* (2005) for the North Sea. As a result, accurate estimates are likely to be site-specific in nature.

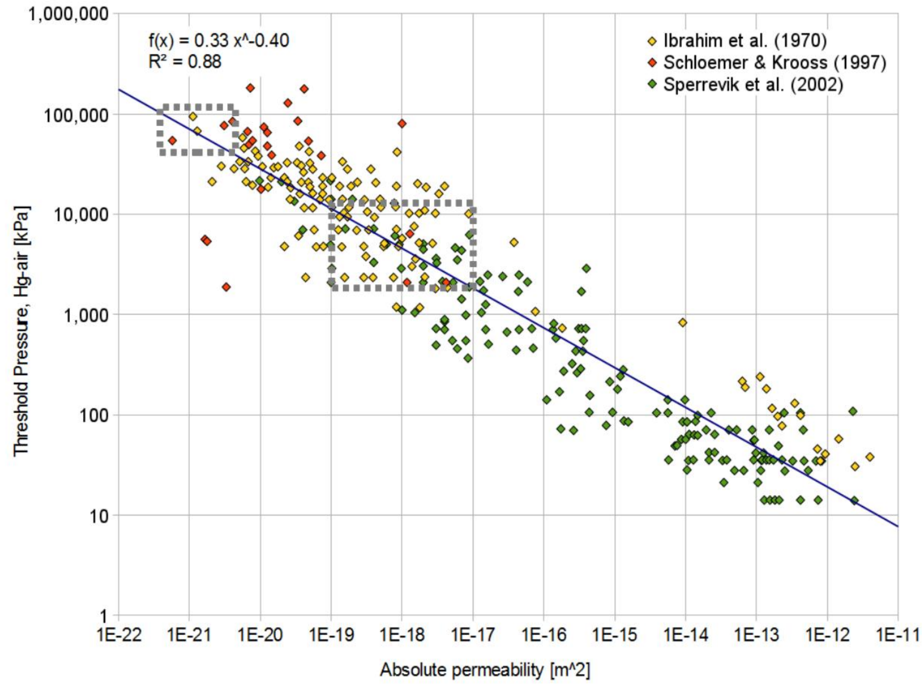

FIGURE 4: An improved power-law transform for the empirical relationship between observed threshold pressure and horizontal permeability in porous media. The data cloud consists of 302 data points collated from 3 published studies. The coefficient of determination, R^2, is high at 0.88, which reflects the coherence of the three largest data sets used (red, yellow and green symbols). The three data sets also extend the range to the nanodarcy spectrum.

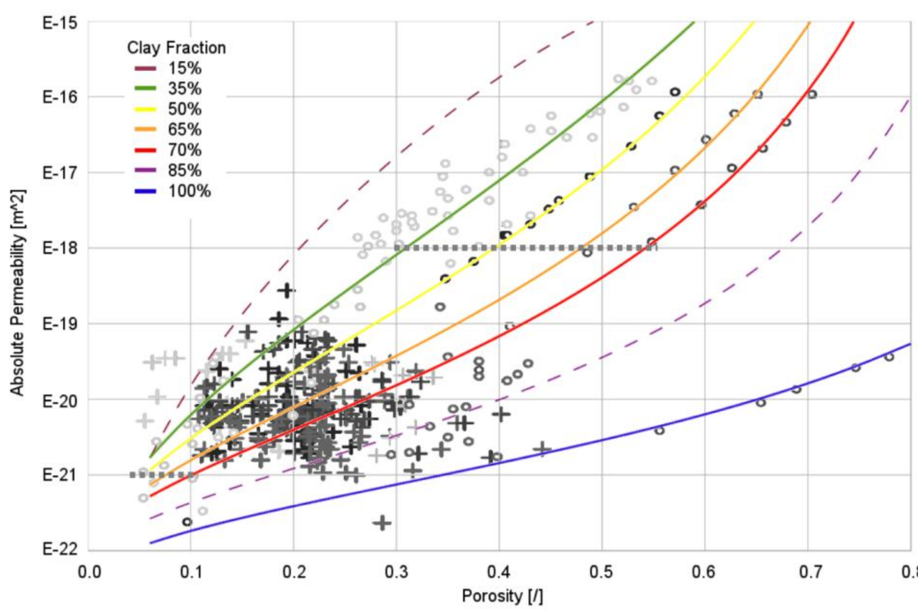

FIGURE 5: The Yang and Aplin (2009) permeability-porosity transform for shales of different clay content. Solid curves are transform matches to the published data. Dashed curves are transform approximations for high-clay and low-clay content shales. The gray lines indicate that a) the high permeability range commonly used in modeling studies (i.e. E-18 m^2, the microdarcy range) may occur over a porosity range of around 30 to 55 percent, i.e. shallow burial conditions; b) the low permeability range (i.e. E-21 m^2, the nanodarcy range) may occur over a porosity range of around less than 10 percent, i.e. much deeper burial conditions. As a first approximation, assuming no scaling issues, the middle ground of 10 to 30% porosity covers a wide spectrum of shales with permeabilities that range from micro-to-nanodarcy but are likely to fall in the middle ground of E-19 to E-20 m^2.

4.5 Porosity-Depth Curves

Poelchau *et al.* (1997) have compiled twenty four published porosity-depth profiles for shales (gray curves) that show the wide range of possible porosities for any given depth. The wide variance is a result of diverse environments, lithological input, and burial history phenomena such as diagenesis, overpressure and erosion. A first order approximation of typical porosity-depth profiles is shown (colored curves) ranging from weak shales with high porosities to tight shales with low porosities (Figure 6). Given the range of possible porosity-depth profiles, accurate estimates of shale porosity, and therefore boundary permeability, will require a regionally-specific geological context.

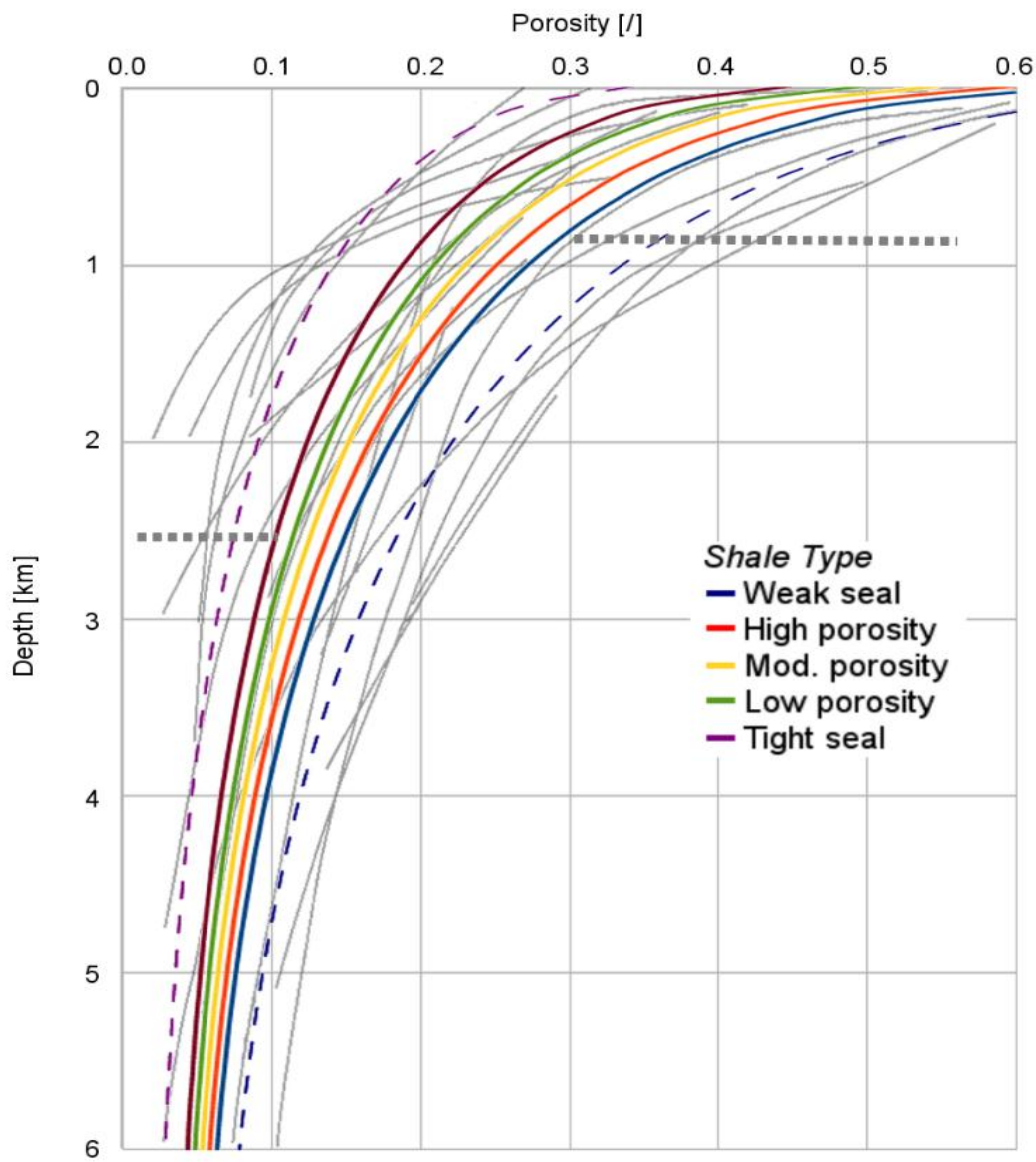

FIGURE 6: Porosity-depth relationships for shales (after Poelchau *et al.*, 1997). The twenty four separate estimates (gray curves) document published literature from 1930-1990. The general approximation (colored curves) represents typical trends in porosity loss. The dashed gray lines indicate that: a) the porosity range associated with microdarcy permeability (30 to 55 percent) typically occurs above 0.8 km depth for an unscaled Yang and Aplin (2009) transform; b) the porosity range associated with nanodarcy permeability (less than 10%) typically occurs at more than 2.5 km depth.

4.6 Scaling the Porosity-Permeability Relationship

The documented empirical relationships (Figures 4-6) are helpful when considering geological flow simulations as they provide an objective measure for extrapolating and interpolating between the typically sparse observations associated with site-specific and regional case studies. As shown, the various attributes (depth-porosity-permeability-threshold pressure) form a chain of interdependent parameters for flow in porous media. However, the validity of these unscaled transform functions needs to be tested by comparison with observed phenomena at the macroscopic scale (e.g. hydrocarbon field column heights and regional pressure distributions).

For example, the regional observations of threshold pressure by Nordgård Bolås *et al.* (2005) provide a scaling context for shales in the North Sea. The threshold pressure range for the hydrocarbon fields and wells studied by Nordgård Bolås *et al.* give an approximate regional range of 5 to 15 MPa (Hg-air) for caprocks at a depth of 2000 to 4000 meters. Although there is considerable complexity in the detail related to faults and fractures, a simple abstraction is to assume that the lowest threshold pressure occurs at the shallowest depth and *vice-versa* (Table 5).

Depth (m)	*Observed Pth (Pa)*	*K from Pth (m^2)*	*Phi from Depth (/)*	*K from Phi (m^2)*	*Scaling factor*
2000	*5,000,000*	*E-18*	*0.15*	*E-20*	*100*
4000	*15,000,000*	*E-19*	*0.08*	*E-21*	*100*

TABLE 5: An upscaling estimate for permeability as represented in the porosity-permeability transform. Assuming modal shale relationships (yellow curve, Figures 5 and 6) for the North Sea, the observed threshold pressures require an scaling factor of 100 to return field-scale permeabilities. *Phi*, porosity; *K*, absolute permeability; *Pth*, threshold pressure. Threshold pressures and depths are estimated from Nordgård Bolås *et al*. (2000).

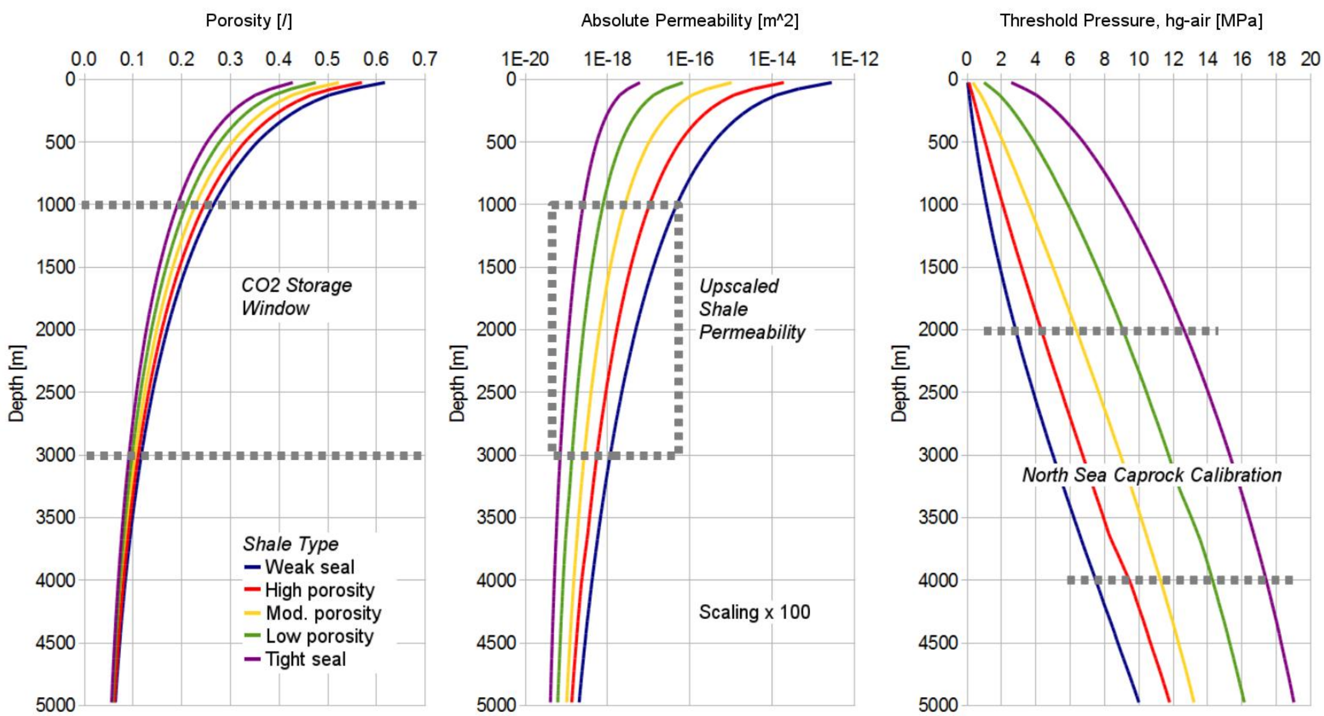

FIGURE 7: Upscaling for regional shale permeability. The depth-porosity-permeability-threshold pressure relationship, as adjusted for the North Sea region, matches the observed threshold pressure relationship (5 MPa at 2000 m; 15 MPa at 4000 m) by upscaling the permeability by two orders of magnitude. The resultant shale curves match the observed caprock behavior and return microdarcy range permeabilities for CO_2 storage depths.

4.7 Faults and Fractures

The previous section describes a regional North Sea example of caprock permeability upscaling. Oil and gas threshold pressures are applied as the calibration data for field-scale permeability. This approach raises the role of fractures and faults on shale-related fluid flow, as regional threshold pressures and permeabilities are strongly dependent on such phenomena. Microfractures, fractures and faults are commonplace in sedimentary rocks at a regional scale, although difficult to directly quantify beyond the seismic expression of faults and direct observation of core samples. The fractal nature of fault distributions implies that the fracture population is much more widely distributed and denser than commonly observed. However, laboratory sampling is understandably biased towards unfractured specimens and the characterization of matrix porosity. Therefore, microscopic and mesoscopic laboratory measurements are unlikely to represent the regional fracture contribution to threshold pressure and permeability despite the fact that, as Bjørlykke (1994) points out, cross-formational flow (i.e. shale-mediated flow) in sedimentary basins is largely controlled by fractures and faults. While recent hydrocarbon basin modeling has addressed the significance of fault and fracture characterization (e.g. Manzocchi *et al.*, 2002; Teige and Hermanrud, 2004; Lothe *et al*., 2005; Sorkhabi and Tsuji, 2005), much uncertainty remains as to how attribute regional shale characteristics that reflect the bulk contribution of fault and fracture populations. However, it is clear that laboratory data needs to be upscaled when applied to field-scale and regional-scale models.

An unscaled comparison of the empirical relationships (porosity-permeability-threshold pressure) illustrates that microdarcy shale permeabilities would only occur at very high matrix porosities and near-surface conditions (i.e. more than thirty percent porosity and less than one kilometer depth). Whereas, hydrocarbon fields within a few kilometers of the surface would have threshold pressures equivalent to column heights measuring thousands of meters. Such extremes are not representative of typical sedimentary basins. To reconcile this discrepancy it has been proposed that either a) a small number of discrete faults control the buoyant fluid retention in hydrocarbon traps or b) the caprock threshold pressure is representative of the background fracture distribution. The fault scenario implies that the threshold pressure for a trap structure is indicative of the fault permeability and not the background caprock threshold pressure nor the regional shale permeability. The fracture scenario implies that the background shale permeability would be a function of the observed threshold pressure. There is evidence for both phenomena in petroleum systems, with some hydrocarbon fields breaching fluid vertically from fault/caprock juxtapositions, whereas other fields breach vertically from the highest structural point despite the presence of faults within the structural closure. With respect to CO_2 storage, the fault scenario would result in low threshold pressures and low shale permeabilities, breaking the inverse correlation between threshold pressure and permeability (a worst case scenario of poor capacity and poor injectivity). The upscaling relationship described in the previous section assumes the fracture scenario. This preserves the threshold pressure-permeability relationship and implies reasonable injectivity and capacity.

4.8 Summary

Various models have been proposed over the last two decades that have simplified the boundary conditions of storage to a closed approximation. Open system models also handle the upper and lower boundaries of deep saline storage as a no-flow approximation. Both approaches reflect either the analytical nature of the solutions or the need to simplify the system to the constraints imposed by numerical simulators when modeling systems at the regional scale. As is evident from the empirical relationships outlined in this section, shale permeabilities for storage environments are likely to fall in the micro-to-nanodarcy range (10^{-17} to 10^{-22} m^2). It follows that the no-flow approximation for boundaries with permeabilities in the microdarcy to nanodarcy range needs to be tested.

5. A Regional Analytical Approach

Analytical models are mathematical abstractions that make a number of simplifying assumptions to render the flow system as a single equation or small group of related equations. This allows for a first approximation of the likely system response to changes in key parameters. A potential shortcoming of analytical models is that they are limited by their simplicity and potentially misleading when considering complex scenarios. If complexity is a significant attribute of the system, numerical simulations are usually required to test the system response. However, changing the modeling paradigm to include permeable shale boundaries is relatively straightforward. The analytical approach needs to address both caprock threshold pressure and permeability, as the need for an effective seal is counterbalanced by maintaining injectivity through natural pressure dissipation. Given the wide range of possible shale permeabilities and the generic nature of the problem, a sensitivity analysis for gas trapping potential and regional brine displacement potential is required. For simple scenarios such as single well problems, homogeneous reservoirs and end-member boundary conditions, both analytical models and numerical simulations need to converge on the same solution, and as such, analytical models provide a critique of numerical simulations and *vice-versa*. For either approach, the validity of the abstraction needs to be tested with real data. As such, these general solutions are an order-of-magnitude approximation. A more detailed analysis requires site-specific data. However, given the generalizations of existing closed system models (e.g. van der Meer and van Wees, 2006; Ehlig-Economides and Economides, 2010) a general approximation is sufficient to assess the merit of the no-flow assumption.

5.1 Regional Trapping Analysis

In the following scenario the trapping potential of a hypothetical regional storage formation is assessed as a function of caprock threshold pressure. The scenario assumes that a limited amount of information is available regarding the storage formation and therefore takes a sensitivity analysis approach to identify potential storage sites. Three scenarios are tested: a weak seal (2 MPa ~ E-17 m^2); moderate seal (5 MPa ~ E-18 m^2); and strong seal (13 MPa ~ E-19 m^2).

- Regional prospect area (60 x 50 km)
- Mapped depth range (1,000 – 3,500 m)
- Storage prospecting window (1,500 – 2,000 m)
- Potential injection locations (50 wells)
- Permeable caprock shale (E-17 to E-19 m^2)
- Threshold pressure range (2 to 13 MPa)

A migration analysis of structural trapping for buoyant CO_2 reveals a number of potential storage sites within the region (Appendix A.2 documents the Young-Laplace equation for buoyant fluid trapping beneath permeable seals). Given the threshold pressure range, the size of the storage sites is strongly dependent on the column height retained by the caprock (Figure 9). Column heights range from around 30 to 200 meters for the three scenarios (Table 6). For the strong seal scenario (13 MPa, Hg-air) the potential plume footprint is equivalent to a giant hydrocarbon field (i.e. hundreds of square kilometers). For a weak seal (2 MPa, Hg-air) plume footprints are much reduced in size, although the largest traps are no smaller than the approximate footprint of the Sleipner plume at a few square kilometers. Four potential storage locations recur. The moderate seal scenario indicates that these locations are large storage prospects for caprock threshold pressures equivalent to microdarcy permeability (5 MPa ~ E-18 m^2).

Caprock Scenario	*Permeability*	*Pth, Hg-air (Pa)*	*Pth, CO_2-H_2O (Pa)*	*Column Height (m)*
Weak seal	*E-17 m^2 / 10 μD*	*2,000,000*	*130,000*	*30*
Moderate seal	*E-18 m^2 / 1.0 μD*	*5,000,000*	*325,000*	*75*
Strong seal	*E-19 m^2 / 0.1 μD*	*13,000,000*	*845,000*	*200*

TABLE 6: A comparison of threshold pressures, related shale permeabilities and column heights for the three trapping scenarios. The column height calculation requires a conversion from the reference system (mercury-air) to the subsurface conditions (carbon dioxide-brine). The conversion assumes an interfacial tension of 28 mN/m (after Bachu and Bennion, 2007), a CO_2 density of 650 kg/m^3 (after Huang *et al*., 1985) and a water density of 1050 kg/m^3.

5.2 Regional Pressurization Analysis

Analytical models of injectivity have been recently reviewed (IEAGHG, 2010). The report notes that the underlying premise for analytical solutions of injectivity is Darcy's law, the relationship between a pressure gradient and the flow rate as a function of fluid viscosity and rock and fluid permeability (Appendix A.3 documents the equation and its common variations in detail). The report notes that a reservoir engineering heuristic for single-phase well flow, as adapted by van Engelenburg and Block (1993) for intra-formational pressure modeling, has been expanded upon in recent years to partially include compressibility, gravitational effects, two-phase flow and relative permeability (e.g. Bickle *et al.*, 2007; van der Meer and Egberts, 2008; Burton and Bryant, 2009; Mathias *et al*., 2009).

Darcy's law, in its simplest form, is a one-dimensional relationship derived in the 19^{th} Century from single-phase pipe flow experiments (Equation 1). As such, the equation describes most hydrodynamic flow in porous media where two and three-dimensional attributes are insignificant. The 'most flow' assumption also implies non-turbulent flow for a single incompressible fluid. For CO_2 storage, if the pressure footprint of a storage site is much larger than the plume volume, the volumetric displacement of brine occurs at a regional scale and, beyond the plume distribution, is a single-phase phenomenon. Furthermore, if the regional pressure regime is hydrostatic and there is no significant hydrodynamic regime prior to injection, the one-dimensional abstraction applies to brine displacement out of the formation and into the surrounding shales, as the principle displacement direction will be orthogonal to the boundary surface in the direction of the pressure drop. Finally, a one-dimensional analysis also requires the storage formation to be relatively thin with respect to the lateral dimensions of the formation, which is usually the case.

Darcy's law can then be adapted for a sensitivity analysis of the pressure footprint associated with the storage of CO_2 in a formation with permeable boundaries, as the shale permeability will allow brine to flow in response to an increase in the storage formation pressure (Equation 2). The equation is re-arranged to consider the boundary surface area required for a given flux (injection rate) as a function of the pressure drop (the difference between the hydrostatic pressure and formation pore pressure) across the boundary layer (caprock and underlying shale thickness).

$$\frac{Q}{A} = -\frac{k}{\mu}\nabla P \qquad\qquad A = -Q\frac{\mu}{k}\frac{L}{\triangle P}$$

EQUATIONS 1 & 2: Darcy's law, in its one-dimensional form, and rearranged for area of flux as a function of flux, pressure change. *A*, boundary surface area; *Q*, injection rate as volumetric flux; μ, brine viscosity; *k*, shale permeability; ΔP, pressure difference; *L*, caprock and underlying shale thickness.

5.3 Worked Example

For example, consider a moderate storage operation into a small confined formation that has a geomechanical limit for injection pressure above hydrostatic. The site is at a depth of 1.5 km flanked above and below by shales that are approximately fifty meters thick. The desired injection rate is a million tonnes of carbon dioxide a year. Assuming an acceptable near-well overpressure of ten megapascals, and an average compartment overpressure of five megapascals, the question is: *what is the minimum shale permeability required for the boundary flux to keep pace with the formation influx and so dissipate brine at the same rate as injection increases the formation fluid volume?*

- A pressure compartment area of 10x10 km: A, 200 km^2 (Upper and lower boundaries)
- An injection rate per well of 1 Mt/yr: Q, 0.05 m^3/s (CO_2 density of 650 kg/m^3)
- A bottom hole fluid pressure of +10 MPa: ΔP, +5 MPa (Pressure compartment average)
- A shale boundary thickness of 50 meters: L, 50 m (Upper and lower shales)
- A brine salinity of 80,000 ppm: μ, 0.5 mPas (Depth ~1.5 km, T ~55ºC, P ~15 MPa)

These conditions allow the shale permeability to be calculated. In this case the boundary layers would need to be 1.25×10^{-18} m^2 or 1.25 µD, equivalent to a threshold pressure of 5 MPa (Hg-air) and a column height of 75 meters.

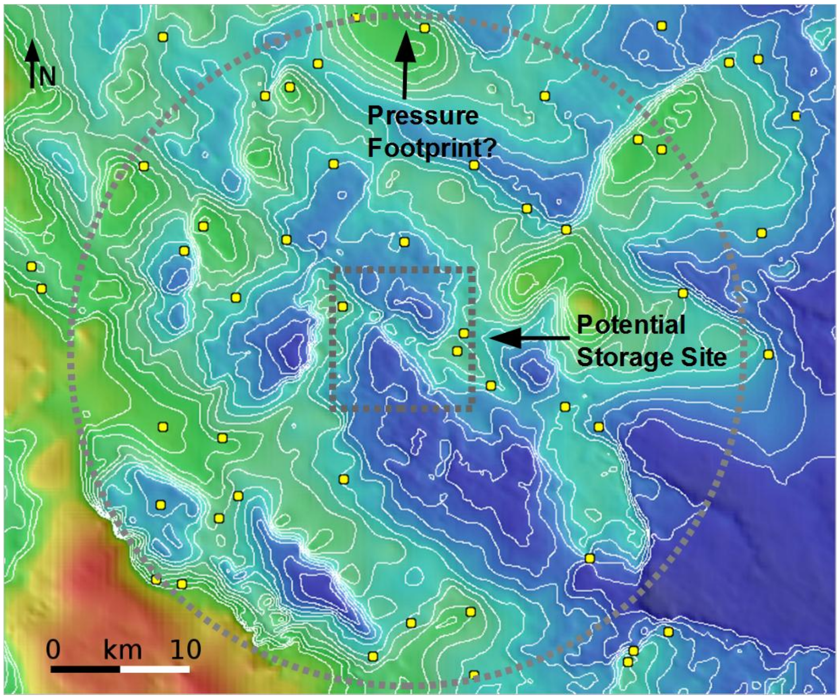

FIGURE 8: Regional caprock map. Uncontoured areas are either too deep or too shallow for storage. The gray dashed box is a 10x10 km square footprint, equivalent to similar plume footprints for current megatonne storage sites (see Figure 1). Fifty wells are distributed within the prospecting fairway (contoured area) to identify the location, size and column height of potential storage sites for different threshold pressure conditions: 2, 5 and 13 MPa (Hg-air). The large dashed gray circle, 50 km diameter, represents a large regional pressure footprint for the hypothetical storage formation.

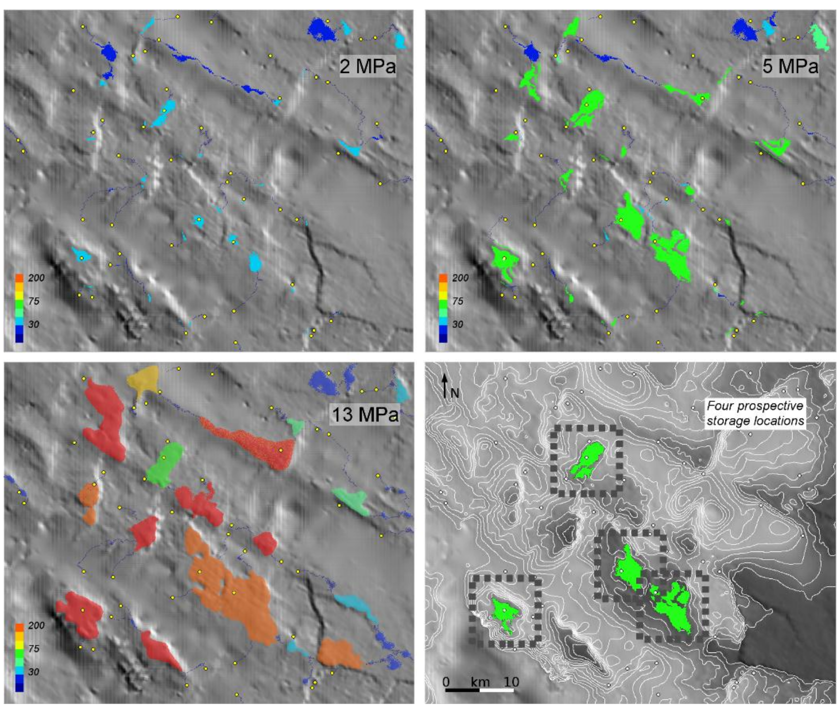

FIGURE 9: A comparison of potential storage locations for the three trapping scenarios. The color bar indicates column heights (0/30/75/200 meters). The summary map shows the four likeliest storage sites (dashed gray boxes) which will be used to consider the pressurization in the following analysis.

5.4 Regional Pressure Footprint, Shale Thickness and Permeability

In the preceding example a very small pressure compartment is assumed, equivalent to a surface area of 200 km^2. This low end of the spectrum is analogous to a compartmentalized formation like the In Salah storage site, where the land surface response and lack of well interference between CO_2 injectors and natural gas producers suggests that the injection wells are isolated in compartments that are pressurizing accordingly (Figure 1). However, most storage operations will be sited in much larger pressure compartments, with the upper end of the spectrum being represented by regional areas measured in thousands of square kilometers (e.g. the Bunter and Utsira Formations, North Sea).

Given the spectrum of possible compartment sizes, a sensitivity analysis is needed to address regional pressurization for reasonable shale permeabilities and boundary layer thickness (Table 7, Figures 10 and 11). The estimated pressure footprint is calculated as an area and expressed as the diameter of a circle centered on the well. The footprint area is calculated from Equation 2. Values in brackets are too large to represent in Figure 10.

Caprock thickness	*Footprint, 10 μD*	*Footprint, 1 μD*	*Footprint, 0.1 μD*
10 m	*3 km*	*8 km*	*25 km*
50 m	*6 km*	*18 km*	*56 km*
100 m	*8 km*	*25 km*	*(80 km)*
200 m	*11 km*	*36 km*	*(113 km)*
500 m	*18 km*	*56 km*	*(178 km)*

TABLE 7: The diameter of pressure footprint circles centered on an injection well with respect to shale thickness (upper and lower boundaries) and shale permeability. The following values are assumed: Injection rate, *Q*, 1 Mt/yr; average footprint pressure increase, *ΔP*, +5 MPa; brine viscosity, *μ*, 0.5 mPas.

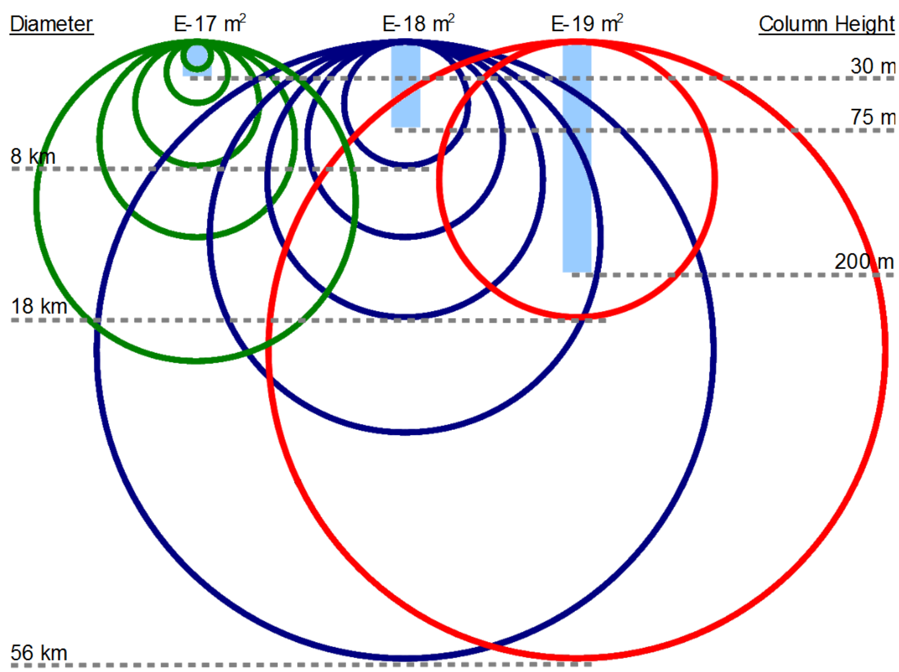

FIGURE 10: Pressure footprint circles and column heights for shale boundaries in the microdarcy range. The circles in each set correspond to the following shale thickness: 10, 50, 100, 200, 500 meters. Note that the column height (and related threshold pressure) is insensitive to shale thickness.

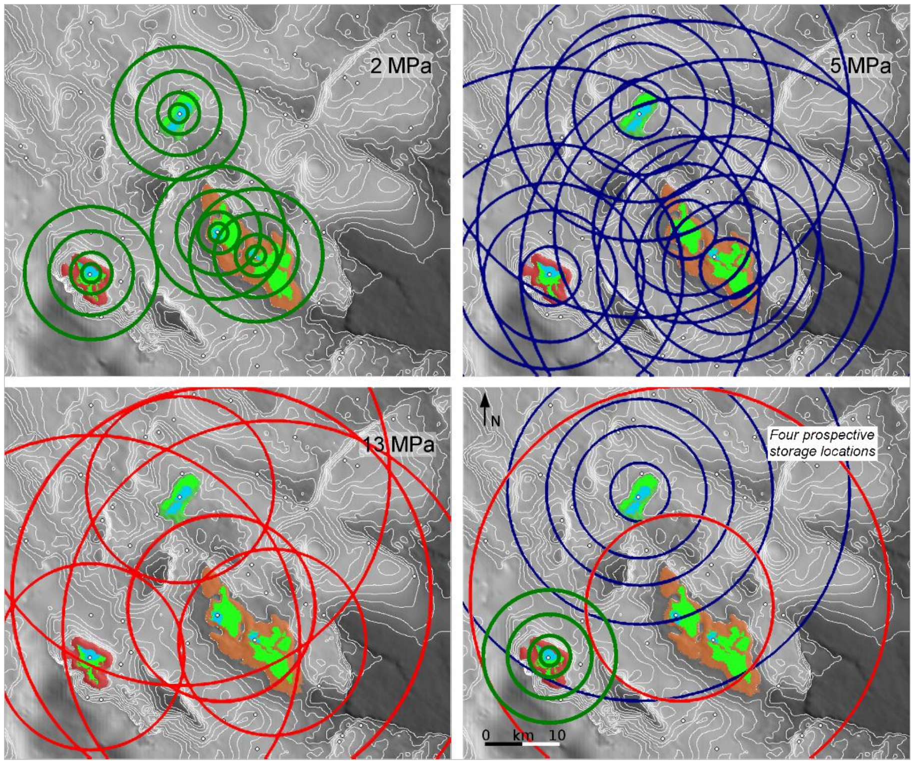

FIGURE 11: A comparison of trapping and pressure footprints for threshold pressures associated with microdarcy range permeabilities. A low threshold pressure (2MPa) and high permeability shale (10 µD, E-17 m^2) results in a small trapping potential (light blue) and a pressure footprint ranging from 3-18 km in diameter for a caprock that is 10-500 meters thick. A high threshold pressure (13 MPa) and low permeability shale (0.1 µD, E-19 m^2) results in giant storage sites (orange) but pressure footprints that are 25-56 km in diameter for a caprock that is 10-50 meters thick, as illustrated in the summary diagram.

The sensitivity analysis reveals that for a relatively modest injection rate of one million tonnes per year, the pressure footprint required to disperse brine through shale boundaries of various thickness, in the microdarcy range, extends from a few kilometers in diameter for a thin and relatively weak seal to tens or possibly hundreds of kilometers for thick and relatively tight seals. Given the following: 1) the apparent sensitivity of the system to shale permeability and boundary layer thickness; and 2), typically poor data constraints and the related order-of-magnitude uncertainty for regional shale permeability estimates, it is clear that it is difficult to predict (beyond a broad approximation) how a storage formation will respond prior to injection (Figure 12). While simple analytical models can provide such an approximation, well constrained numerical simulations are required to test these outcomes. To review, the following points arise with respect to the regional analysis of shale-bounded storage formations:

- The pressure footprint size is highly sensitive to both the shale permeability and boundary layer thickness.
- The threshold pressure, column height, and related capacity are insensitive to shale thickness.
- The pressure response will be strongly affected by the compartment size and related boundary surface area.
- An effective combination of storage capacity and injectivity appears to occur over a narrow depth window.
- Microdarcy permeability will be specific to regional shale properties such as clay content and burial history.
- Within reason, thin shales provide better pressure dissipation without decreasing the caprock trap potential.
- The optimal storage scenario is a regionally thin shale unit with microdarcy permeability.
- Regional shale permeability characterization is likely to have a high degree of uncertainty.
- Analytical models cannot account for features such as faults, erosional unconformities and gas chimneys.

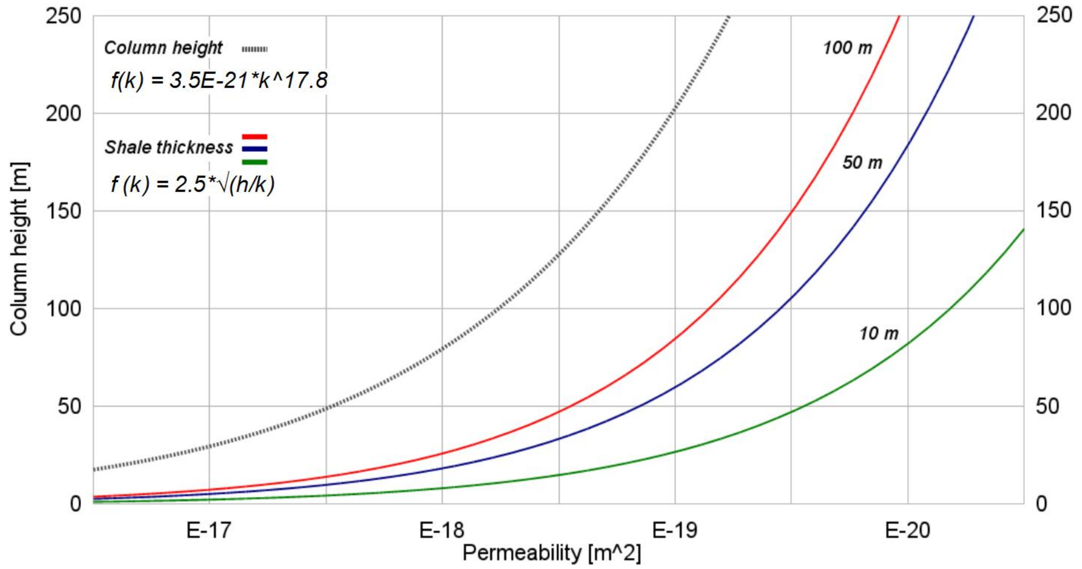

FIGURE 12: Power law relationships for column heights and pressure footprints. The column height, *f(k)*, for a given density contrast between CO_2 and brine (400 kg/m^3), is a function of the permeability, *k*. The diameter of the pressure footprint, *f(k)*, for an average pressure increase of 5 MPa, is proportional to the square root of the boundary layer thickness, *h*, and the inverse square root of the permeability, *k*.

6. Storage Site Analysis

Given the relationships established in the previous sections, it is possible to run a hypothetical case study for a storage site to consider the various contributions of solubility, compressibility and permeability (Figure 13). The test site is a moderate structural trap (180 km^2 in area and 2 km^3 in volume) that spills to the south-east for a column height of 30 meters. The storage formation is a high net-to-gross sandstone that is 25 meters thick.

- *Formation:* *sandstone*
- *Thickness:* *25 m*
- *Porosity:* *0.22*
- *Permeability:* *300 mD*
- *Trap depth:* *1500 m*
- *Spill point:* *1530 m*
- *Trap area:* *180 km^2*
- *Compartment:* *375 km^2*
- *P and T:* *15.5 MPa, 55ºC*
- *Brine density:* *1050 kg/m^3*
- *CO_2 density:* *650 kg/m^3*
- *Gas saturation:* *0.68*

The storage site is located within a small pressure compartment that is about twice the area of the trap at 375 km^2. Rock and water compressibility estimates (Figure 2) allow the pore volume and brine volume changes within the trap to be estimated (Table 8).

Volume	*(Total)*	*Uncompressed*	*Compressed*	*Change*	*(New total)*
Compartment	*1.00*	*9.3750 km^3*	*9.37500000 km^3*	*0.00%*	*1.00*
Formation rock	*0.78*	*7.3125 km^3*	*7.29421875 km^3*	*0.25%*	*0.77805*
Formation brine	*0.22*	*2.0625 km^3*	*2.05837500 km^3*	*0.20%*	*0.21956*
Compression	*0.00*	*0.0000 km^3*	*0.02240625 km^3*	*7.42% of the trapped CO_2*	
Trapped CO_2	*0.145**	*0.2992 km^3*	*0.30185200 km^3*	*0.89% increase in capacity*	

TABLE 8: Compression estimates for a 200 Mt storage site within a small compartment (volume ~ 9 km^3; rock volume ~ 7 km^3; brine volume ~2 km^3). Water compression: 0.2%, ΔP, +5 MPa, CW, 4E-10/Pa; Rock compression: 0.25%, ΔP, +5 MPa, CR, 5E-10/Pa. * Storage coefficient.

6.1 Compressibility Contribution

As a first approximation, the compressibility contribution to storage capacity appears to be relatively small. An average 5 MPa pressure increase changes the trap capacity by less than 1 percent, whereas the pressure compartment compression contributes to around 7 percent of the total potential CO_2 capacity. For a CO_2 density of 650 kg/m^3:

- The capacity changes from 195 to 197 megatonnes due to a 1% compression change in the trap's pore space.
- A fraction of the potential trap capacity, around 15 megatonnes, results from compartment compression.

In this example, the compression response for a small compartment provides a few years of storage before the compressibility limit is reached, assuming that the pressure limit is no higher than a few megapascals for a reasonable fracture gradient. The trap structure (as defined by the structural closure, spill point and column height) is only slightly affected by compression with respect to the total potential capacity.

6.2 Solubility Contribution

For this analysis, the solubility contribution during injection is assumed to be limited to the brine within the pore space associated with the plume, as described in section 2.5. For a porewater saturation of 32%, the estimate for the saturated brine contribution is less than three percent of the total CO_2 mass injected (Table 2):

- The potential capacity increases from about 197 to 203 megatonnes due to a 3% solubility contribution.

For this example, the solubility contribution is a few megatonnes at most, although this is dependent on the site filling completely, and as such, will only be reached incrementally. For a compressibility limit of 15 megatonnes capacity, the solubility contribution would be less than a megatonne. Compressibility and the space available for compression are clearly the dominant factors in the absence of brine displacement. Recent pressure cell models (e.g. Heinemann, 2010) that infer a significant compressibility contribution require large regional formations like the Bunter Sandstone. In this example the pressure compartment is relatively small. The middle ground is potentially a decade or more of reasonable injectivity before the compression limit is reached. These findings, in the absence of brine displacement and pressure dissipation, are in accord with similar published closed system approximations.

6.3 Permeability Contribution

The final part of the analysis considers the shale properties necessary for natural pressure dissipation. Given the site characteristics, it is possible to estimate the injection rate, Q, and brine displacement for different shale boundaries:

• A pressure compartment area of 375 km^2:	A, 750 km^2	(for upper and lower boundaries)
• A shale permeability in the microdarcy range:	k, 10^{-17} to 10^{-19} m^2	(for the regional shale boundaries)
• An average overpressure of +5 MPa:	ΔP, +5 MPa	(for the pressure compartment average)
• A shale boundary thickness of 50 meters:	L, 50 m	(for both the upper and lower shales)
• A brine salinity of 80,000 ppm:	μ, 0.5 mPas	(1.5 km depth, T ~ 55ºC, P ~ 15.5 MPa)

The injectivity of the hypothetical site is highly sensitive to the boundary conditions. Fifty meter thick microdarcy shales allow for an injection rate of 3 megatonnes per year via natural brine displacement. This scenario provides about 60 years of storage capacity for a 400MW power station. A weak shale has a sufficient seal for storage (30 meter column height) and provides very high injection rates (30 Mt/yr), i.e. similar to Sleipner where no pressurization is observed and indications are that the formation could take much higher rates.

Boundary layer	*Permeability*	*Permeability*	*Boundary flux*	*Injection rate*
Weak shale	10^{-17} m^2	*10 microdarcy*	*1.5* m^3/s	*30 Mt/yr*
Moderate shale	10^{-18} m^2	*1 microdarcy*	*0.15* m^3/s	*3 Mt/yr*
Tight shale	10^{-19} m^2	*0.1 microdarcy*	*0.015* m^3/s	*0.3 Mt/yr*

TABLE 9: Injection rates for microdarcy shale permeabilities, assuming a boundary layer thickness of 50 meters and injection rate of 1 Mt/yr ~ 0.05 m^3/s.

A tight shale scenario limits the injection rate to 0.3 Mt/yr, i.e. similar to rates observed at In Salah, which is currently injecting into three small fractured and faulted compartments. A nanodarcy range (10^{-20} to 10^{-22} m^2) would cause injectivity to fail. No industrial-scale project has reported this type of pressure response.

- More than 95% of the capacity, at around 195 megatonnes, is dependent on the boundary conditions, with respect to surface area, shale permeability and layer thickness.
- An order-of-magnitude approximation for injectivity is around 0.1 to 10 Mt/yr for the microdarcy range (10^{-17} to 10^{-19} m^2), a boundary thickness of 10 to 100 meters, and a high regional pressure change (5MPa).
- The test case was a moderate sized trap (10x18 km) in a small pressure compartment (15x25 km). Larger compartments within regional formations increase the boundary surface area, lowering the pressure change.
- A closed system zero-flux assumption is a fair approximation for small compartments that are bounded by reasonably thick shales in the nanodarcy range (10^{-20} to 10^{-22} m^2).

Note that the storage coefficient is high at 14.5 percent (Table 8). A second scenario with a much larger pressure compartment (36x60 km), equivalent to the expected storage coefficient of 2.5 percent, increases the injectivity by approximately an order of magnitude and the compression contribution to 43 percent of capacity (Appendix A.5).

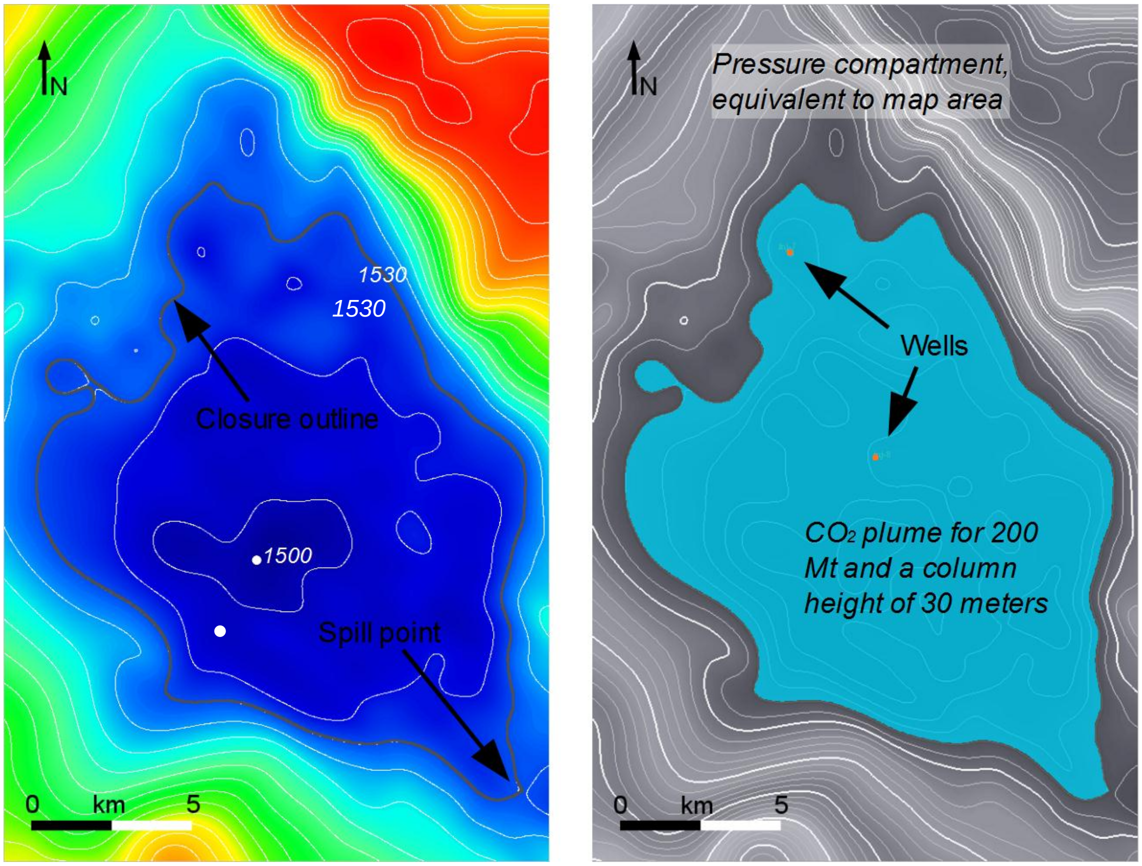

FIGURE 13: A storage site model. The depth range is 1.5-1.7 km. The structural closure (gray line) spills to the south east for a 30 meter column of CO_2. The simulated storage capacity is approximately 200 megatonnes, with two injection well locations (orange circles) on the flank and crest.

7. Storage Site Simulation

A single-phase hydrodynamic simulation allows for a simple validation test of the analytical solution. The single-phase numerical approach addresses the flux balance at the boundary of the formation required to displace an equivalent volume of brine to that of injected CO_2 (Appendix A.6). The simulation is not intended to address the plume distribution, which requires a two-phase simulation that would encompass relative permeability and capillary pressure. The single phase approximation deploys a high resolution hydrodynamic solver and accurate pressure field modeling (Figure 14). With respect to boundary conditions, the edge boundaries of the model are open to allow for brine displacement. The baffle effect of the shales that surround a storage formation, and the closed system approximation, is then handled by buffering the edge of the storage compartment with a shale frame. The frame is a kilometer wide along the lateral edges of the model, and twenty meters thick at the upper and lower faces. The large aspect ratio is required as the assumed permeability anisotropy of shales (10:1) requires a much thicker lateral buffer to prevent edge effects when simulating the pressure response associated with pressure dissipation for a thin regional formation within a hydrostatic context. In the test case scenario, the storage formation is overlain and underlain by fifty meter thick shales and twenty meter thick sandstone formations. The initial pressure condition is hydrostatic. For the initial run, the storage formation is a high net-to-gross sandstone (porosity: 20%, permeability, 300 mD). The second series of simulations considers a heterogeneous storage formation (Figure 15), based on the *10th SPE comparative solutions dataset No.2* benchmark description of a shallow marine sandstone (Christie and Blunt, 2001).

7.1 Initial Conditions

The hydrodynamic simulation differs mathematically from the one-dimensional Darcy analysis described in the previous section. The simulated hydrodynamic flow is in three dimensions, and calculated as a function of the governing equation for pressure diffusion, i.e. a standard Laplacian approximation (Bear, 1972). This combines mass conservation with Darcy's law. As such, the underlying premise remains the same, and both the analytical and numerical approaches should be similar. The hydrodynamic model tests the following: a) does the numerical solution converge with the analytical solution; and b) as a first approximation, does the formation heterogeneity significantly change the pressure distribution and brine flux. The initial conditions of the model are as follows:

Input	*SI Units*	*English Units*	*Input*	*SI Units*	*English Units*
Model area:	*17x27 km*	*(~11x17 miles)*	*Temperature at datum:*	*55 °C*	*(122 °F)*
Shale permeability:	*10^{-18} m^2*	*(1 µD)*	*Brine density:*	*1,050 kg/m3*	*(75,000 ppm)*
Caprock depth, datum:	*1,500 m*	*(4,920 ft)*	*Injection interval:*	*2x10 m*	*(2x33 ft)*
Pressure at datum:	*15.5 MPa*	*(2,175 psi)*	*Bottom hole pressure:*	*+10 MPa*	*(3,700 psi)*

TABLE 10: Initial conditions for the simulation. The settings are comparable to the analytical solutions of the previous section. The model area has increased to include the shale baffles that allow for a closed system approximation within an open system simulation.

7.2 Simulated Pressure Distribution

The simulation results indicate that for the scenario described (50 meter thick shale layers with microdarcy permeability), the pressure equilibrates within decades (Figures 16 and 17). The inter-well pressure field (7 MPa) reflects the high well pressure (10 MPa), while the far-field (SE corner) stabilizes at about 3 MPa, resulting in a steady state injection rate of about 2.7 Mt/yr and an average compartment pressure increase of 5 MPa (Figure 17). This result is in accord with the analytical solution that indicated a maximum injectivity of 3 Mt/yr for an equilibrium pressure of 5 MPa. While the pressure field is fairly insensitive to the heterogeneity within the formation, the flow response picks out highly permeable channels. This well-known dichotomy implies that pressure relief wells will need to be placed carefully to avoid CO_2 breakthrough.

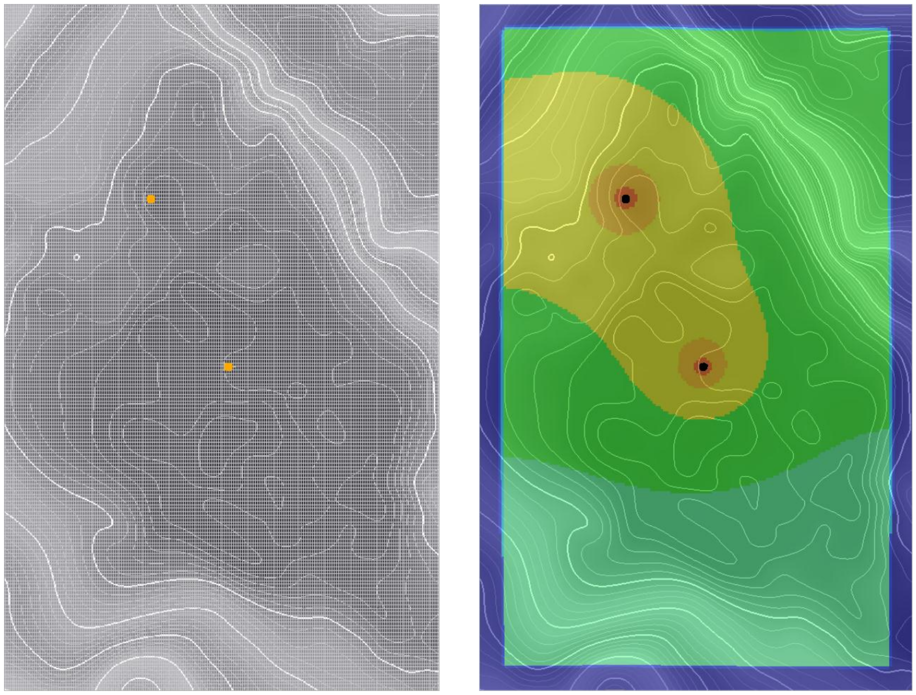

FIGURE 14: Numerical simulation mesh, viewed from above, for the hydrodynamic model (5,875,200 cells, 18 layers, 50x50x5 meter resolution). The panel on the right shows the steady state pressure distribution for a 10 MPa well pressure above hydrostatic. The average pressure increase is 5 MPa.

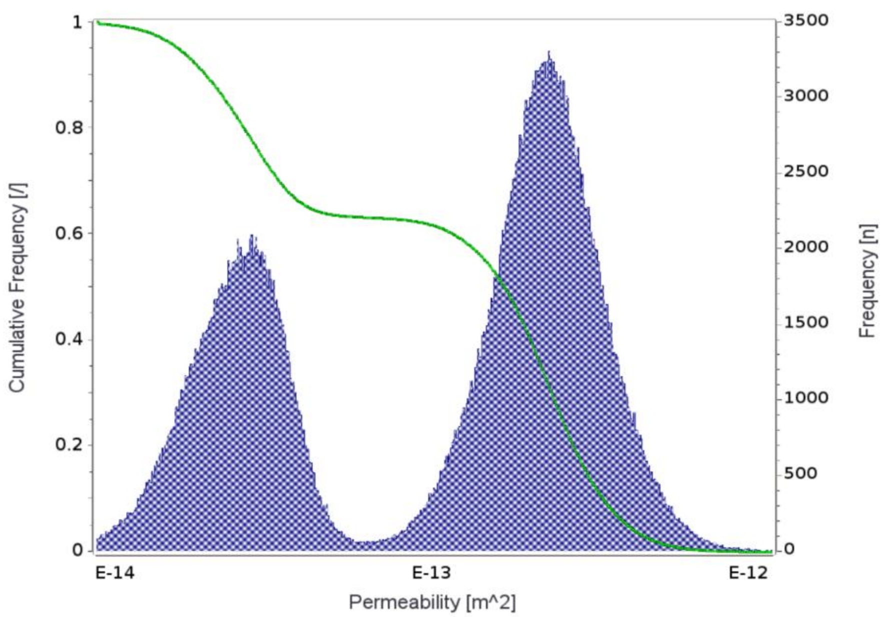

FIGURE 15: Porosity distribution for the heterogeneous storage formation scenario. A log-normal bimodal distribution for high and low quality formation lithologies (300 mD and 30 mD). The spectrum covers sub-darcy sandstones and supra-microdarcy siltstones, discretized as ten lithologies for the mesh.

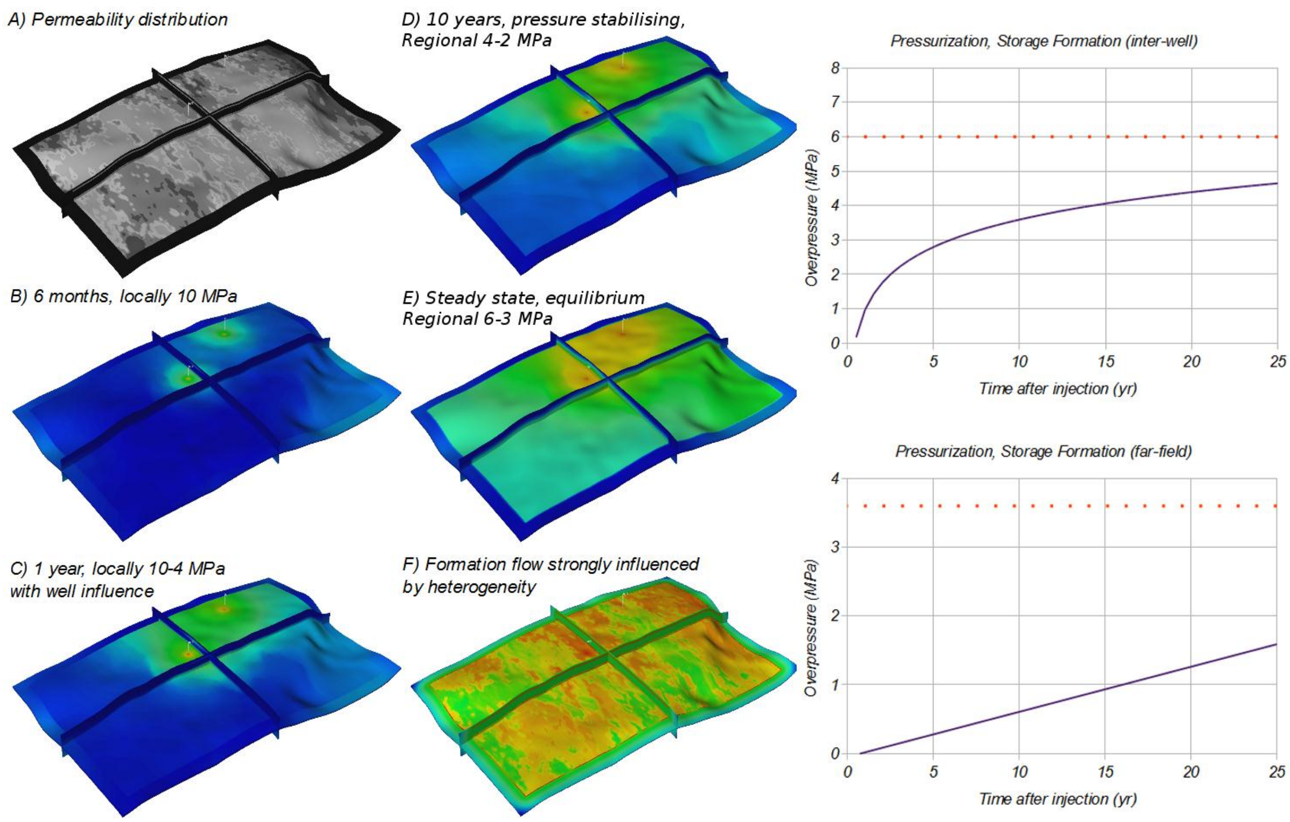

FIGURE 16: Simulation results for the heterogeneous formation scenario. Vertical exaggeration: x20. The pressure distribution (B-E) blushes out evenly from the injection wells despite the heterogeneity, eventually equilibrating within decades for an average pressure increase of 5 MPa. By contrast, the brine flux within the formation is sensitive to the permeability distribution, strongly favoring permeable channels over lower permeability sections. The graphs chart the pressure increase over the first twenty five years between the wells (natural log) and at 10 km from the wells (linear) in the SE corner of the model. The charted trends indicate that the near- and far-field will approach equilibrium (95% of steady state, red dashed line) within 50 to 60 years.

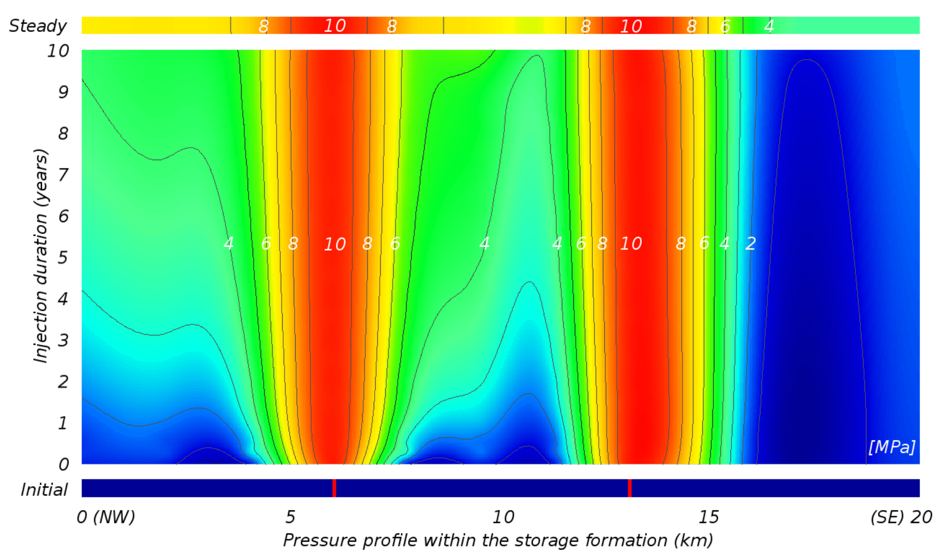

FIGURE 17: Formation pressure versus time. The color bars (top and bottom) represent the initial conditions and steady state solution (10 MPa at the wells; 5 MPa average pressure regionally). The middle panel shows the pressure evolution over 10 years along a 20 km section through the wells (NW-SE).

7.3 Brine Displacement Flux Rates

The flux rates and brine displacement behavior of the formation and boundary shale are reported at steady state conditions for the numerical simulation (Figure 18). The boundary flux through shales is of the order of millimeters per year, while the reservoir flux is meters per year, although poor quality reservoir sections (equivalent to intra-formational shales) behave in a similar fashion to the boundary layers.

- Boundary Shales: the average brine flux rate within the boundary layer shales is low at around 1 mm/year and fairly evenly distributed, with a small but noticeable increase within a few kilometers of the well, resulting in an approximate doubling of the flux rate to around 2 mm/year directly above the well. This reflects the ratio of injection well pressure to average regional pressure (10:5 MPa). These flux rates allow the boundary shales to displace an equivalent volume of brine-to-CO_2 into the stratigraphy above and below the formation.

- Storage Formation: brine flux rates within the storage formation are much higher and directly related to well proximity and formation permeability. The maximum flux rate occurs within the immediate vicinity of the injection wells for high permeability reservoir intervals that intersect the well (10 to 100 m/yr within approximately a 2 km radius of the well). The flow rates drop to around 1 m/yr within a few kilometers of the well for areas of high reservoir quality, and are as low as 0.01 to 0.001 m/yr in areas of poor reservoir quality.

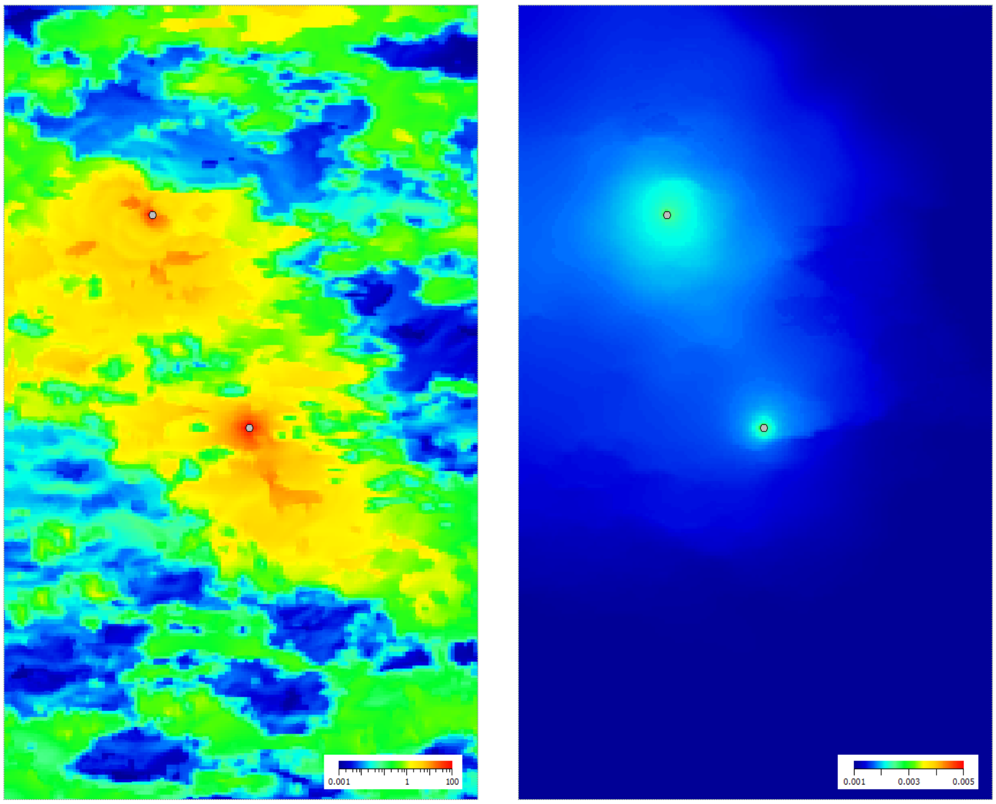

FIGURE 18: Numerical simulation outputs for brine flux within the storage formation and the shale boundary layer. Flux rates within the storage formation average around 1 m/yr but are highly variable (note the logarithmic scale), depending on well proximity and reservoir permeability. The flux rates within the shale are much lower at around 1 mm/yr, and more uniform (note the non-logarithmic scale), with a doubling of flux rate over the injection wells.

These results reflect the aims of the model design: a) the heterogeneous storage formation, to test the sensitivity of brine flux to reservoir quality variation within a storage formation; and b) the homogeneous shale boundaries to test the results of the analytical model for a regional shale seal with microdarcy permeability.

With respect to shale heterogeneity, while it is difficult to generalize on flux rates (shale variation is site-specific in nature and difficult to gather data on), natural heterogeneity will likely result in localized flux variations over several orders of magnitude, as observed in the flux rate response to reservoir heterogeneity. However, two further scenarios are worth considering with respect to flux and brine displacement: a) well-related flow; and b) fault-related flow. A simple Darcy's law approximation can be used to estimate the likely outcome for these scenarios (Table 11).

Scenario A - Leaking well		*Scenario B - Leaking Fault*	
• *Area associated with the fractures:*	*A, 10* m^2	• *Area associated with the fractures:*	*A, 100,000* m^2
• *Fractured caprock permeability:*	*k,* 10^{-15} m^2	• *Fractured caprock permeability:*	*k,* 10^{-16} m^2
• *Pressure within the vicinity of the well:*	*ΔP, +5 MPa*	• *Pressure within the vicinity of the fault:*	*ΔP, +5 MPa*
• *Caprock thickness:*	*L, 50 m*	• *Caprock thickness:*	*L, 50 m*
• *Brine viscosity:*	*μ, 0.5 mPas*	• *Brine viscosity:*	*μ, 0.5 mPas*
• *Brine density:*	*ρ, 1050* kg/m^3	• *Brine density:*	*ρ, 1050* kg/m^3
• *Flux rate at well:*	*q ~ 6 m/yr*	• *Flux rate at fault:*	*q ~ 0.6 m/yr*
• *Brine displacement at well:*	*Q ~ 66,000 kg/yr*	• *Brine displacement at fault:*	*Q ~ 66 kt/yr*

TABLE: 11: Potential brine displacement for two scenarios: a) leaking well and b) leaking fault. For the first scenario, an abandoned well within a few kilometers of the injection wells has a millidarcy permeability associated with fractures in the surrounding shale. For the second scenario, a 10 km fault within a few kilometers of the injection wells has a sub-millidarcy permeability (0.1 mD) associated with a fracture zone that is 10 m thick.

In the case of the leaky fault, the fault-related area accounts for approximately 0.01% of the closed system boundary area (100,000 m^2 vs. 754 km^2) but accounts for about 1% of the flux. In the case of the leaky well, the well-related area is a much smaller fraction: 0.000001% of the boundary area (10m^2 vs. 754 km^2). The leaky well flux is also small at around 0.0001% of the total flux. While these are crude approximations, the mass balance indicates the significant role that well and fault-related fracture characterization will play in estimating the potential impact of brine displacement on shallow potable resources. This aspect of brine displacement will be addressed in a forthcoming IEAGHG study on far-field and shallow impacts of brine displacement, scheduled for 2011.

8. Summary and Conclusions

Concerns regarding pressurization and brine displacement have been largely model driven. The scarcity of pressure data for existing megatonne injection projects, and the reasonable injectivity of these sites to date, has meant that pressure prediction for deep saline formation storage has tended to be analytical in nature, with published models relying on hypothetical ranges and conceptual constraints for likely scenarios. Chief amongst the constraints have been the assumptions concerning the likely boundary conditions of deep saline formations. Given the relatively low permeability of shales in comparison to other common sedimentary rocks (with the exception of salt), an understandable abstraction has been the ‘no-flow’ boundary assumption for the large upper and lower surfaces of regional storage formation models. This simplifies the modeling approach for both open and closed systems and lends itself to simple analytical solutions. However, the ‘no-flow’ assumption for shales is a poor approximation. The following points summarize how this has led to extreme pressurization scenarios with respect to CO_2 storage:

- Early research outlined the three principal components of a pressurizing system: CO_2 solubility, system compressibility, and shale permeability.

- Recent research indicates that solubility, on injection timescales, contributes very little to pressure relief. Furthermore, system compressibility will only relieve pressurization in the largest regional formations. Boundary layer permeability is, therefore, the critical component for pressure in most storage scenarios.

- The first analytical and numerical models abstracted storage formations as either open or closed systems. In these early models, for open and closed approximations, the vertical boundaries are handled as no-flow zero-permeability barriers. However, for most storage formations, these upper and lower barriers are permeable shales. The no-flow approximation was assumed to be reasonable given the low permeabilities of shales.

- An objective assessment of common shale permeabilities indicates a microdarcy-to-nanodarcy range (10^{-18} to 10^{-21} m^2). A comparison of laboratory data to regional observations indicates that permeability requires upscaling. This upscaling effect needs to be constrained by site-specific calibration data. For the North Sea, the regional upscaling factor is approximately two orders of magnitude.

- It appears that regional permeabilities in the microdarcy range (10^{-18} m^2) are likely for a storage depth window of 1-3 km. While nanodarcy permeabilities (10^{-21} m^2) will result in a closed system response that is akin to a zero-flow boundary model, microdarcy permeabilities are sufficient to provide natural pressure dissipation for deep saline formations. Indeed, shale permeabilities in excess of a microdarcy will effectively result in an open system pressure response. However, the trapping potential of such shales will be poor, due to a low threshold pressure (permeability and threshold pressure are co-dependent).

In the absence of data, modeling is, at best, a sensitivity analysis for likely scenarios. The model results presented here are in accord with recent work presented elsewhere, most notably by Zhou *et al.* (2008) and Birkholzer *et al.* (2009). However, this study is intended to add to that understanding by placing the various closed system model approaches in context, and also by examining the published permeability relationships for shales that critique the underlying assumptions of the earlier published models. General relationships for shales indicate that all but the smallest deep saline formations will experience significant natural pressure dissipation as a result of brine displacement into the surrounding strata via shale-mediated flow, assuming approximately microdarcy shales.

For regional formations, the zero-flow boundary approximation is only valid for very small pressure compartments and regional shales with permeabilities in the nanodarcy range. General relationships indicate that, for microdarcy shale permeabilities, the storage potential of deep saline formations probably exceeds the capacity and injectivity requirements of CO2 storage, although very small compartments may require water abstraction strategies.

Appendices

A.1 Pressure

Pressure is a fundamental aspect of geological flow. Blaise Pascal (1623-1662) pioneered the scientific term in the 17th Century, having measured atmospheric pressure while investigating phenomena observed by Galileo (1564-1642) and Torricelli (1608-1647). For geological systems, as a first approximation, pressure gradients control single phase flow (Darcy's law, 1855). Threshold pressures control two-phase trapping (Young-Laplace equation, 1805).

For a perfectly closed system, the pressure response within a formation is principally a function of compressibility (e.g. Morris and Johnson, 1967). The retardation of water flow in mudstones and other low permeability rocks also results in the development of elevated regional formation pressures, as evident in petroleum systems (Law and Spencer, 1998). It is believed that high rates of CO_2 injection may induce regional pressurization. The near-well pressure limit for injection is reasonably well constrained by the fracture gradient of a caprock or formation. The regional limit on an extensive pressure footprint is more arbitrary in that 1) the pressure field may interfere with neighboring storage operations, and 2) the pressure field may encounter a significant change in caprock integrity (faults, fractures, facies, and wells) that lowers the pressure limit for a site. High formation pressures may also displace brine to shallower formations and, potentially, contaminate potable aquifers.

A.2 Threshold Pressures

The Young-Laplace equation for threshold pressure is derived from the work of two polymaths during the late European Enlightenment. Thomas Young (1773-1829) a London physician, and leading light in the coffee house research of that period, published *An Essay on the Cohesion of Fluids* (1804) regarding empirical wetting angle-interfacial tension relationships and capillary phenomena. Pierre-Simon Laplace (1793-1864), a French aristocrat and astronomer, theoretically described the pressure change across an interface for a free surface as a function of capillary radii and interfacial tension, published in *Mécanique Céleste* (1806). The German mathematician, Carl Friedrich Gauss (1777-1855), refined and unified this earlier work, resulting in a combined expression. As a result, the Young-Laplace equation had emerged by the early 20th century (e.g. *Encyclopaedia Britannica*, 1911). The equation describes the capillary pressure difference sustained across an interface between two fluids, such as oil and water, as a result of surface tension (Equation 3). The pressure difference is related to the shape of the surface at the interface.

$$\Delta P = 2\gamma H = \gamma\,(1/r1 + 1/r2) \qquad [3]$$

A familiar variation of the Young-Laplace equation is the description of capillary flow in porous media (e.g. Washburn, 1921). This relates the pore size distribution to capillarity (Equation 4). Another popular expression of the Young-Laplace equation relates the gravitationally stable column height of an oil or gas trap to the capillarity (e.g. Hobson, 1954) by exchanging the capillary pressure term with a function of density, column height and standard gravity (Equation 5). Recent research has investigated the time-dependent nature of saturation in porous media as a function of interfacial tension kinetics (Tuck *et al.*, 1997). However, the phenomenon is limited to a timescale of seconds-to-days, and so does not impact on macroscopic phenomena such as CO_2 injection or hydrocarbon migration.

$$Pc = 2\gamma.\cos\theta/r \qquad [4]$$

$$\Delta\rho gh = 2\gamma.\cos\theta/r \qquad [5]$$

Pc, the pressure due to capillary forces; γ, the interfacial tension; θ, the contact angle of the wetting fluid with the substrate; r, the capillary radius for the largest pore throat; $\Delta\rho$, the density difference between the formation waters and trapped hydrocarbons; g, standard gravity; h, the stable column height. Substituting the threshold pressure for the capillary pressure derives the maximum potential column height for a trap. This may be reduced by a spill point.

A.3 Pressure Gradients

Darcy's law is a continuum approximation for pressure gradients in porous media. The law was posthumously derived from, and named after experiments undertaken by the engineer Henry Darcy (1803-1858) and Charles Ritter. (1793-1864). The pipe flow experiments for water and highly porous sand introduced the concept of permeability to earth sciences and fluid flow. The experiments did not explicitly observe viscosity or derive intrinsic permeability. However, the formulas published within the treatise on the fountains of Dijon, France (Darcy, 1856) are precursors of the law as it is commonly known today, that established the proportionality of single phase volumetric flux for a given area to a falling pressure head in the direction of flow. The constant of proportionality that Darcy ascribed to this relationship is equivalent to the modern usage of hydraulic conductivity.

Darcy's law is a phenomenologically-derived constitutive equation describing macroscopic flow in porous media. The darcy unit, 'D' (equivalent to 9.869233e-13 m^2 or approximately 1 μm^2) was assigned in the 1930s (Wyckoff *et al.,* 1933). The unit abbreviation is occasionally written as 'd' and 'D', although the wider scientific convention is for honorific letters to be capitalized, such as joule (J) and newton (N). The law describes the flux for a given area as a function of the porous medium's intrinsic permeability and the fluid's viscosity in response to a negative pressure gradient. The law is an expression of the conservation of momentum that was later derived theoretically from first principles using the later Navier-Stokes equation (Hubbert, 1953).

The Navier-Stokes equations are derivations of Newton's second law: conservation of momentum. These reasonably complex differential equations conserve mass, momentum and energy for fluid motion and are notable for their application to turbulent systems such as weather, aerodynamics and the motion of stars within galaxies. Darcy’s law can be obtained by volume-averaging the simpler steady-state Stokes equation that assumes low inertia relative to viscosity.

Darcy's law, in its original form (Equations 6-9) is only valid for single-phase viscous flow with a Reynolds number less than about 10. For higher Reynolds numbers, the onset of turbulence impedes the flow in addition to viscosity. Extrapolations of the original law are used to describe multi-phase flow through porous media, especially in the field of petroleum engineering.

$Q/A = -\nabla P.k/\mu$	The simplest expression, one dimension	[6]
$K = \begin{matrix} kxx & kxy & kxz \\ kyx & kyy & kyz \\ kzx & kzy & kzz \end{matrix}$	Permeability tensor	[7]
$Q/A = -\mathrm{K}(\nabla \mathrm{P}-\rho g\hat{e}z)/\mu$	Single phase flow, three dimensions	[8]
$q = Q/A$	Flux, aka Darcy velocity	[9]

Darcy's law and its derivatives use macroscopic measures of average rock and fluid properties: intrinsic permeability and viscosity. Intrinsic permeability, also known as absolute permeability, is a property of the porous medium. The viscosity term refers to the dynamic viscosity or absolute viscosity of an incompressible Newtonian fluid (Pas). Kinematic viscosity is the ratio of a fluid's dynamic viscosity to its density (m^2/s). Bulk or volume viscosity applies for compressible Newtonian fluids. The macroscopic approach is an aspect of continuum mechanics. The original experiment was for water flow in saturated sand:

- *Saone* sand, 1-2 mm grain size
- Single phase, fresh water
- High permeability, 38% porosity
- High flux, with the onset of turbulence

For a Darcy flow model of hydrocarbon migration, it is assumed that the hydrocarbons migrate as a separate phase (e.g. Hubbert, 1953; Bear, 1972). This is supported by the observation that oil and water do not mix. However, the assumption that the Darcy flow domain extends to low flux rates has been challenged by the alternative paradigm of invasion percolation. A precise mass balance model for both approaches requires that the dissolution and diffusion of light hydrocarbons in formation waters be accounted for. For multi-phase flow, Darcy's law is modified to introduce the concept of relative permeability. Absolute permeability is independent of the pore fluid, assuming that there is no reaction between the rock and the fluid. The effective permeability of a specific immiscible fluid where more than one phase is present is lower than the absolute permeability. The relative permeability is the effective permeability normalized relative to the absolute permeability (Equation 10).

k	the absolute permeability of the rock	
ko	the effective permeability for oil	
$kro = ko/k$	the relative permeability for oil	[10]

Hubbert (1953) proposed a phase-specific variation to describe the buoyant flow of oil (Equation 11). Sylta (1993) adapted this variation to devise a Darcy-based ray tracing algorithm for buoyant flow. Bear (1972) formulated a composite equation (Equation 12) that includes buoyancy ($\rho g\hat{e}z$), capillary forces (Pc) and relative permeability (kr). Bear (1972) attempts to reconcile Darcy's law (Equation 13) with the Young-Laplace equation (Equation 14), although a deconstruction of this approach shows that it is not possible to reconcile the expressions of threshold pressure and capillarity with Darcy's law without forcing the mathematics (e.g. Schneider, 2003). Upscaling for composite algorithms requires the adjustment of the permeability, relative permeability and capillary pressure.

$$Qo/A = -K(\rho w - \rho o) g\hat{e}z.(kro/\mu o) \quad [11]$$
$$Qo/A = -K(\nabla(Pw+Pco) - \rho o g\hat{e}z).(kro/\mu o) \quad [12]$$
$$Q/A = -K(\nabla P - \rho g\hat{e}z)/\mu \quad [13]$$
$$Pth = 2\gamma.\cos\theta/r \quad [14]$$

KEY: Equation 11) Oil phase, buoyancy (after Hubbert, 1953). Equation 12) Phase-specific, combined with capillarity (after Bear, 1972). Equation 13) Darcy's law, single phase. Equation 14) Young-Laplace equation.

A.4 Single Well Heuristic

A common flow-rate equation for CO_2 injection (van Engelenburg and Blok, 1993) that appears as part of many open and closed analytical models is based upon a reservoir engineering heuristic for possible gas extraction flow rates. The principle assumption is that the formation has zero-flux boundaries vertically (for open systems the formation is also assumed to be horizontally infinite). The second assumption is that the formation is homogeneous and isotropic, resulting in symmetrical radial flow. The third assumption is that injection does not increase the reservoir pressure.

$$Q_s = \Delta P_{wb}\,(2\pi kh\rho_r) / (\rho_s \ln(r_e/r_w)\mu_r \quad [15]$$

Q_s	[m^3/s]	Flow rate under standard conditions (15°C and 100 kPa, SPE Metric)			
ΔP_{wb}	[Pa]	Effective pressure (bottom hole well pressure – reservoir pressure)			
ρ_r ρ_s	[kg/m^3]	CO_2 density (reservoir conditions and standard conditions)			
μ_r	[Pa.s]	CO_2 viscosity (reservoir conditions)			
r_e	[m]	Radius, range of influence	k	[m^2]	Formation permeability
r_w	[m]	Radius of the well	h	[m]	Formation thickness

A.5 Storage Site Analysis, Scenario 2

A second scenario for the storage site analysis considers the contributions of solubility, compressibility and permeability with respect to a larger pressure compartment. The test site remains a structural trap (180 km^2 in area and 2 km^3 in volume) that spills to the south-east for a column height of 30 meters. The storage formation also remains a high net-to-gross sandstone that is 25 meters thick. However, in this scenario the storage site is located within a larger pressure compartment (36x60 km, 2160 km^2, 54 km^3) that results in a storage efficiency factor of approximately 2.5 percent for the trap with respect to its regional context (i.e. the expected regional storage coefficient for a sandstone formation (P50~ 2.5% – Table 3). Rock and water compressibility estimates are calculated as before (Table 11).

Volume	*(Total)*	*Uncompressed*	*Compressed*	*Change*	*(New total)*
Compartment	1.00	54.000 km^3	54.00000 km^3	0.00%	1.00
Formation rock	0.78	42.12 km^3	42.01470 km^3	0.25%	0.77805
Formation brine	0.22	11.88 km^3	11.85624 km^3	0.20%	0.21956
Compression	0.00	0.0000 km^3	0.129060 km^3	42.8% of the trapped CO_2	
Trapped CO_2	0.025*	0.2992 km^3	0.30185200 km^3	0.89% increase in capacity	

TABLE 11. Water and rock compression estimates for a 200 Mt site within a large pressure compartment (volume ~ 54 km^3; rock volume ~ 42 km^3; brine volume ~ 12 km^3). Water compression: 0.2%, ΔP, +5 MPa, CW, 4E-10/Pa; Rock compression: 0.25%, ΔP, +5 MPa, CR, 5E-10/Pa. * Storage coefficient.

Compressibility contribution. The compressibility contribution increases to almost half the trap capacity for the larger pressure compartment. For an average 5 MPa pressure increase, the trap capacity increase remains the same at less than 1 percent, whereas the pressure compartment compression contributes to around 84 Mt or 43 percent of the total potential CO_2 capacity.

Solubility contribution. This would be the same as for the first scenario at about 3% or a 6 Mt increase to 203 Mt.

Permeability contribution. The larger pressure compartment significantly increases the surface area for natural pressure dissipation. The possible injection rates, *Q*, for different shale boundaries are as follows (Table 12).

- A pressure compartment area of 2,160 km^2: A, 4,320 km^2 (for upper and lower boundaries)
- A shale permeability in the microdarcy range: k, E-18 to E-22 (for the regional shale boundaries)
- An average overpressure of +5 MPa: ΔP, +5 MPa (for the pressure compartment average)
- A shale boundary thickness of 50 meters: L, 50 m (for both the upper and lower shales)
- A brine salinity of 80,000 ppm: μ, 0.5 mPas (1.5 km depth, T ~ 55ºC, P ~ 15.5 MPa)

Boundary layer	*Permeability*	*Permeability*	*Boundary flux*	*Injection rate*
Moderate shale	E-18 m^2	1.0 microdarcy	0.864 m^3/s	20 Mt/yr
Tight shale	E-19 m^2	0.1 microdarcy	0.086 m^3/s	2 Mt/yr
Very tight shale	E-20 m^2	10 nanodarcies	0.009 m^3/s	0.2 Mt/yr

TABLE 12. Injection rates for microdarcy shale permeabilities, assuming a boundary layer thickness of 50 meters and injection rate of 1 Mt/yr ~ 0.05 m^3/s.

A.6 Model Assumptions

The analytical models presented in this report follow common assumptions for heuristic pressure models:

- Firstly, the system is abstracted to one dimension. This allows for an application of Darcy`s law in its simplest form. The critical assumption here is that the lateral boundary contribution in a closed system approximation is minimal. The reasoning for this is based on the much larger surface area of the vertical boundaries relative to the lateral boundaries.
- Secondly, the system is abstracted to a single phase (brine). This avoids the onerous complexities of two-phase flow (e.g. relative permeability). The critical assumption here is that the phenomenon of interest, pressure change, occurs over a large regional area (single-phase regime) relative to the near-well plume distribution (two-phase regime).
- Thirdly, the compressibility and solubility contributions are estimated as a first approximation. This establishes that the likely pressure-relief component from these aspects of the system is small (a few percent relative to the much larger pore water displacement contribution for microdarcy shale boundaries), and so justifies the simple one-dimensional Darcy flow heuristic used to assess the size of the pressure footprints.
- Fourthly, the analytical pressure footprints are expressed as circles of a given diameter centered on the injection well. While storage compartments are highly unlikely to be circular in shape, this approach allows the required surface area necessary for pressure dissipation to be assessed, and the overlapping of pressure footprint circles for neighboring wells indicates the likelihood of inter-well pressure influence.
- Finally, the analytical solution employs an average pressure for the pressurized region, in order to establish the average pressure increase and area required to displace brine at the boundaries of the compartment, assuming a certain shale permeability and thickness. In reality, the maximum allowable pressure in the system will occur at the injection well, and decrease in an approximately radial fashion away from the injection well, as a function of the local and regional permeability, as well as influence of neighboring injection wells. This much more complex analysis is more suited to a numerical simulation, which can then be compared to the simple analytical solution with respect to the average pressure increase in the simulated compartment.

The numerical simulations presented in this report employ the following approximations:

- Firstly, the model domain is a small storage compartment (15x25 km) relative to the much larger areas of regional deep saline formations like the Utsira and Bunter Formations, North Sea. Small storage compartments are more likely to result in pressurization due to the smaller surface area of the system.
- The storage compartment is laterally buffered by one kilometer thick shales, and vertically buffered by 50 meter thick shales. This allows the simulation to run with open system `Dirichlet` boundary conditions, while the pressure system is baffled laterally and vertically by low permeability shales, resulting in a more realistic closed system scenario than a no-flow `Neumann` boundary approximation.
- The lateral boundary thickness (1 km) is chosen to prevent the pressure dissipation reaching the open system edge of the model domain prior to it reaching the thin sandstone reservoirs (20 m thick) that flank the upper and lower boundary shales (50 m thick). This reflects the typical proximity of reservoir units above and below a deep saline formation (tens-to-hundreds of meters) relative to the lateral separation between such formations (several kilometers). The permeability anisotropy of the shales (horizontal-to-vertical = 10:1) means that a vertical pressure influence of 50 meters is equivalent to a lateral influence of 500 meters. Hence, the lateral boundary is sufficiently thick to buffer the flow without edge effects.
- Shale heterogeneity is not considered, as there is currently a poor understanding of regional shale facies distributions. Furthermore, the heterogeneity of regional shales is typically associated with faults and fracture clusters such as gas chimneys. These have not been addressed as such features are typically site-specific.

References

Bachu, S. and Bennion, B. 2007. Effects of in situ conditions on relative permeability characteristics of CO_2 brine systems. *Environmental Geology*, **54**, 1707-1722.

Bachu, S., Gunter, W. D. and Perkins, E. H. 1994. Aquifer Disposal of CO_2: Hydrodynamic and Mineral Trapping. *Energy Conversion & Management*, **35**, 269-279.

Bear, J. 1972. *Dynamics of Fluids in Porous Media.* Elsevier, New York, 1-569.

Bergman P. D. and Winter, E. M. 1995. Disposal of carbon dioxide in aquifers in the US. *Energy Conversion & Management*, **36**, 523–526.

Bickle, M., Chadwick, R. A., Huppert, H. E., Hallworth, M. & Lyle, S. 2007. Modeling CO_2 Accumulation at Sleipner: Implications for Underground Carbon Storage. *Earth & Planetary Science Letters*, **255**, 164 – 176.

Birkholzer, J. T., Zhou, Q., Tsang, C.-F. 2009. Large-scale impact of CO_2 storage in deep saline aquifers: a sensitivity study on pressure response in stratified systems. *International Journal of Greenhouse Gas Control*, **3**, 181-194.

Bjørlykke, K. 1994, Fluid flow and diagenesis in sedimentary basins. In: Parnell, J. (Ed.) *Geofluids: origin, migration and evolution of fluids in sedimentary basins*. Geological Society of London, Special Publication, **78**, 127-140.

Bredehoeft, J.D. and Hanshaw, B. B. 1968. On the Maintenance of Anomalous Fluid Pressures: I. Thick Sedimentary Sequences. *GSA Bulletin*, **79**, 1097-1106.

Bredehoeft, J. D., Neuzil, C. E. and Milly, P. C. 1983. Regional flow in the Dakota aquifer: a study of the role of confining layers. *U.S. Geological Survey Water Supply Paper 2237*, pp 45.

Bredehoeft, J. D., Wesley, J. B. and Fouch T, D. 1994. Simulations of the origin of fluid pressure, fracture generation, and the movement of fluids in the Uinta Basin, Utah. *AAPG Bulletin*, **78**, 1729-1747.

Budyko, M. I. 1969. The effect of solar radiation variations on the climate of the Earth. *Tellus*, **21**, 611–619.

Bunney, J. R. and Cawley, S. J. 2007. *Evaluation of CO_2 Storage Capacity, Leakage Mechanisms and Injector Well Placement in a Giant Oilfield at Late Stage of Production*, AAPG Hedberg Research Conference on Basin Modeling Perspectives: Innovative Developments and Novel Applications, The Hague, Netherlands, 6-9 May.

Burton, M. and Bryant, S. L. 2009, Eliminating buoyant migration of sequestered CO_2 through surface dissolution: implementation costs and technical challenges. *SPE Reservoir Evaluation and Engineering*, **12**, 399-407.

Callendar, G. S. 1938. The Artificial Production of Carbon Dioxide and Its Influence on Climate. *Quarterly Journal of the Royal Meteorological Society*, **64**, 223-240.

Cavanagh, A. J., Haszeldine, R. S. and Blunt, M. J. 2010. Open or Closed? A discussion of the mistaken assumptions in the Economides pressure analysis. *Journal of Petroleum Science and Engineering*, **74**, 107-110.

Chadwick, R. A., Noy, D. J. and Holloway, S. 2009. Flow processes and pressure evolution in aquifers during the injection of supercritical CO_2 as a greenhouse gas mitigation measure, Petroleum Geoscience, **15**, 59–73.

Christie, M. A. and Blunt, M. J. 2001. Tenth SPE Comparative Solution Project: A comparison of Upscaling Techniques. *SPE Reservoir Evaluation and Engineering*, **4**, 308-317.

Corbet, T. F. and Bethke, C. M. 1992. Disequilibrium fluid pressures and groundwater flow in the western Canada sedimentary basin. *Journal of Geophysical Research*, **97**, 7203-7217.

CSLF. 2008. *Comparison Between Methodologies Recommended for Estimation of CO_2 Storage Capacity in Geological Media – Phase III Report*. Carbon Sequestration Leadership Forum, pp 21.

DeGroot, M. H. 1987. A Conversation with George Box. *Statistical Science*, **2**, 239-258.

Deming, D. 1994. Factors necessary to define a pressure seal. *AAPG Bulletin*, **78**, 1005-1009.

Deming, D. and Nunn, J.A. 1991. Numerical simulations of brine migration by topographically driven recharge. *Journal of Geophysical Research*, **96**, 2485–2499**.**

Doughty, C. and Pruess, K. 2004. Modeling Supercritical Carbon Dioxide Injection in Heterogeneous Porous Media. Vadose Zone Journal, **3**, 837–847.

Ehlig-Economides, C. A. and Economides, M. J. 2010. Sequestering Carbon Dioxide in a Closed Underground Volume. *Journal of Petroleum Science and Engineering*, **70**, 123-130.

Garven, G. 1989. A hydrogeologic model for the formation of giant oil sands deposits of the Western Canada sedimentary basin. *American Journal of Science*, **289**, 105-166.

Hassanzadeh, H., Pooladi-Darvish, M., Elsharkawy, A. M., Keith, D. and Leonenko, Y. 2007. Predicting PVT data for CO_2–brine mixtures for black-oil simulation of CO_2 geological storage. *International Journal of Greenhouse Gas Control*, **2**: 65-77.

He, Z., and Corrigan, J. 1995. Factors necessary to define a pressure seal: discussion: *AAPG Bulletin*, **79**, 1075-1078.

Heinemann, H. 2010. *CO_2 Storage Capacity in the Bunter Sandstone Limited by Local Pressure Development, UK Southern North Sea*. Carbon Storage Opportunities in the North Sea, Geological Society, 24-25 March.

Hobson, G. D. 1954. *Some fundamentals of petroleum geology*. Oxford University Press, London, 1-139.

Holloway, S., Noy, D. J. and Chadwick, R. A. 2009. *Modeling CO_2 Injection into the Bunter Sandstone, UK Sector of the Southern North Sea*, Deep Saline Aquifers for Geological Storage of CO_2 and Energy, IFP, France, 27-29 May.

Huang, F., Li, M., Lee, L. and Starling, K. 1985. An accurate Equation of State for CO_2. *Journal of Chemical Engineering of Japan*, **18**, 490-496.

Hubbert, M. K. 1953. Entrapment of petroleum under hydrodynamic conditions. *AAPG Bulletin*, **37**, 1954-2026.

IEAGHG, 2009. *Development of Storage Coefficients for CO_2 Storage in Deep Saline Formations*. IEA Greenhouse Gas R&D Programme, 2009/13, pp 118.

IEAGHG, 2010. *Injection strategies for CO_2 storage sites*. Prepared by the Cooperative Research Centre for Greenhouse Gas Technologies, Canberra, IEA Greenhouse Gas R&D Programme, 2009/14 pp 1-90.

IPCC, 2005. Metz, B., Davidson, O., de Coninck, H., Loos, M. and Meyers, L. (Eds.). *Special Report on Carbon Dioxide Capture and Storage*. Intergovernmental Panel on Climate Change. Cambridge University Press, UK, pp 143. www.ipcc.ch/publications_and_data/publications_and_data_reports_carbon_dioxide.htm, accessed on April 17, 2010.

Keeling, C. D. 1978. The Influence of Mauna Loa Observatory on the Development of Atmospheric CO_2 Research. In: Miller, J. (Ed.) *Mauna Loa Observatory: A 20th Anniversary Report.* NOAA Special Report, 36-54.

Law, B. E. and Spencer, C. W. 1998. Abnormal Pressures in Hydrocarbon Environments. *AAPG Memoir*, **70**, 1-11.

le Gallo, Y. 2008. Post-closure migration for CO_2 storage and regional pressure. *Energy Procedia*, **1**, 3259-3266.

Lothe, A. E., Borge, H. and Sylta, Ø. 2005. Evaluation of late caprock failure and hydrocarbon entrapment using a linked pressure and stress simulator. In: Boult, P. and Kaldi, J. (Eds.) *Evaluating Faults and Cap Rock Seals, AAPG Hedberg Series*, ***2***, 163-178.

Luo, X. R., Yan, J. Z., Zhou, B., Hou, P., Wang, W. and Vasseur, G. 2008. Quantitative estimates of oil losses during migration, Part II. *Journal of Petroleum Geology*, **31**, 179-190.

Manzocchi, T., Heath, A. E., Walsh, J. J. and Childs, C. 2002. The representation of two phase fault-rock properties in flow simulation models. *Petroleum Geoscience*, **8**, 119-132.

Mathias, S. A., Hardisty, P. E., Trudell, M. R. and Zimmerman, R. W. 2009. Screening and selection of sites for CO_2 sequestration based on pressure buildup. *International Journal of Greenhouse Gas Control*, **3**, 577-585.

Morris, D. A. and Johnson, A. I. 1967. *Physical properties of rock and soil materials, as analyzed by the Hydrologic Laboratory of U.S. Geological Survey 1948-1960.* Geological Survey Water Supply Paper, 1839-D.

MRCSP, 2010. R. E. Burger Plant, Shadyside Ohio Midwest Regional Carbon Sequestration Partnership. http://216.109.210.162/AppalachianBasin.aspx, accessed on April 17, 2010.

Muggeridge, A., Abacioglu, Y., England, W. and Smalley, C. 2005. The rate of pressure dissipation from abnormally pressured compartments. *AAPG Bulletin*, **89**, 61–80.

Neuzil, C. E. 1986. Groundwater flow in low-permeability environments. Water Resources Research, **22**, 1163-1195.

Newman, G. H. 1973. Pore Volume Compressibility of Consolidated, Friable, and Unconsolidated Reservoir Rocks Under Hydrostatic Loading. *Journal of Petroleum Technology*, **25**, 129-134.

Nordgård Bolås, H. M., Hermanrud, C. and Teige, G. M. G. 2005. The Influence of Stress Regimes on Hydrocarbon Leakage. In: Boult, P. and Kaldi, J. (Eds.) *Evaluating Faults and Cap Rock Seals, AAPG Hedberg Series*, ***2***, 109-124.

Nicot, J.-P. 2008. Evaluation of large-scale CO_2 storage on fresh-water sections of aquifers: An example from the Texas Gulf Coast Basin. *International Journal of Greenhouse Gas Control*, **2**, 582-593.

Oruganti, Y. and Bryant, S. L. 2010. *Evolution of a Pressure-Induced Risk Management Strategy for CO_2 Injection in Deep Saline Aquifers*. AAPG Annual Convention, April 11-14, 2010, New Orleans, Abstract.

Pacala, S. and Socolow, R. H. 2004. Stabilization Wedges: Solving the Climate Problem for the Next 50 Years with Current Technologies. *Science*, **305**, 968–972.

Peterson, I. 2004. *Flight of the bumblebee*. Science News Online. sciencenews.org/ articles/ 20040911/ mathtrek.asp, accessed on April 17, 2010.

Poelchau, H. S., Baker, D. R., Hantschel, T. H., Horsfield, B. & Wygrala, B. 1997. Basin simulation and the design of the conceptual basin model. In: Welte, D. H., Horsfield, B. & Baker, D. R. (Eds.) *Petroleum and basin evolution: insights from petroleum geochemistry, geology and basin modeling*. Springer Verlag, 5-70.

Purcell, W. R. 1949. Capillary pressure - their measurements using mercury and the calculation of permeability therefrom. *AIME Petroleum Transactions*, **186**, 39-48.

Rapaka, S., Chen, S., Pawar, R. J., Stauffer, P. H. and Zhang, D. 2008. Non-modal growth of perturbations in density-driven convection in porous media. *Journal of Fluid Mechanics*, **609**, 285-303.

Rasool, S. I. and Schneider, S. H. 1971. Atmospheric Carbon Dioxide and Aerosols: Effects of Large Increases on Global Climate. *Science*, **173**, 138-141.

Rowe, A. M. and Chou, J. C. S. 1970. Pressure-Volume-Temperature-Concentration Relation of Aqueous NaCl Solutions. *Journal of Chemical Engineering Data*, **15**, 61–66.

Rutqvist J., Birkholzer J., Cappa F., and Tsang C.-F. 2007. Estimating Maximum Sustainable Injection Pressure during Geological Sequestration of CO_2 using Coupled Fluid Flow and Geomechanical Fault-slip Analysis. Energy Conversion and Management, **48**, 1798–1807.

Schneider, F. 2003. Modeling multiphase flow of petroleum at the sedimentary basin scale. *Journal of Geochemical Exploration*, **79**, 693-696.

Sorkhabi, R., and Tsuji, Y. 2005. The Place of Faults in Petroleum Traps. In: Sorkhabi, R., and Tsuji, Y. (Eds.) Faults, Fluid Flow and Petroleum Traps. *AAPG Memoir*, **85**, 1-31.

Spycher, N., Pruess, K. and Ennis-King, J. 2003. CO_2–H_2O mixtures in the geological sequestration of CO_2. I. Assessment and calculation of mutual solubilities from 12 to 100 8C and up to 600 bar. *Geochimica Cosmochimica Acta*, **67**, 3015–3031.

Sylta, O. 1993. New techniques and their applications in the analysis of secondary migration. In: Doré, A. G., Augustson, J. H., Hermanrud, C., Stewart, D. J. and Sylta, O. (Eds.) *Basin Modeling; Advances and Applications; Proceedings of the Norwegian Petroleum Society Conference*. Norwegian Petroleum Society.

Swarbrick, R E, Osborne, M. J., Grunberger, D., Yardley, G. S., Macleod, G., Aplin, A. C., Larter, S. R., Knight, I. and Auld, H. A. 2000. Integrated study of the Judy Field (Block 30/7a) - an overpressured Central North Sea oil/gas field. Marine and Petroleum Geology, 17, 993-1010.

SCCS, 2010. Benchmarking worldwide CO_2 saline aquifer injections. Eds Aleksandra Hosa, A. Esentia, M., Stewart, J. Working paper 2010/3. www.sccs.org.uk/publications.html, accessed on April 17, 2010.

Teige, G. M. G. and Hermanrud, C. 2004. Seismic characteristics of fluid leakage from an underfilled and overpressured Jurassic fault trap in the Norwegian North Sea. *Petroleum Geoscience*, **10**, 35-42.

Thibeau, S. and Mucha, V. 2009. *Have we overestimated saline aquifer CO_2 storage capacity?* Deep Saline Aquifers for Geological Storage of CO_2 and Energy, IFP, France, 27-29 May.

Tóth, J. 1963. A theoretical analysis of groundwater flow in a small drainage basin. *Journal of Geophysical Resources*, **68**, 4795-4812.

Tuck, D. M., Bierck, B. R. and Jaffe, P. R. 1998. Synchrotron radiation measurement of multiphase fluid saturations in porous media: Experimental technique and error analysis. *Journal of Contaminant Hydrology*, **31**, 231-256.

USDOE, 2008. *Carbon Sequestration Atlas of the United States and Canada*. U.S. Department of Energy National Energy Technology Laboratory Office of Fossil Energy, pp 90.

USDOE, 2009. *Small-Scale Carbon Sequestration Field Test Yields Significant Lessons Learned*. U.S. Department of Energy, Fossil Energy Techline. http://fossil.energy.gov/news/techlines/2009/09031, accessed on April 17, 2010.

USDOE, 2010. *Carbon Sequestration Atlas of the United States and Canada*. U.S. Department of Energy National Energy Technology Laboratory Office of Fossil Energy, pp 90.

van Engelenburg, B. C. W. and Blok, K. 1991. *Prospects for the Disposal of Carbon Dioxide in Aquifers*, Dept. of Science, Technology and Society, University of Utrecht, Rep. No. G-91006.

van Engelenburg, B. C. W. and Blok, K. 1993. Disposal of carbon dioxide in permeable underground layers: A feasible option? *Climatic Change*, **23**, 55-68.

van der Meer, L. G. H. 1992. Investigations regarding the storage of carbon dioxide in aquifers in the Netherlands. *Energy Conversion & Management*, **33**, 611–618

van der Meer, L. G. H. 1995. The CO_2 storage efficiency of aquifers. *Energy Conversion Management*, **36**, 513-518.

van der Meer, L. G. H. and van Wees, J. D. 2006. Limitations to Storage Pressure in Finite Saline Aquifers and the Effect of CO_2 Solubility on Storage Pressure. *Society of Petroleum Engineers*, SPE 103342, pp 9.

van der Meer, L. G. H. and Egberts, P. 2008. Calculating subsurface CO_2 storage capacities. *The Leading Edge*, **27**, 502-505.

Washburn, E. W. 1921. The Dynamics of Capillary Flow. *Physical Review*, **17**, 273 - 283.

Wyckoff, R. D., Botset, H. G., Muskat, M. and Reed D. W. 1933. The measurement of the permeability of porous media for homogeneous fluids. *Review of Scientific Instruments*, **4**, 395.

Yamamoto, H., Zhang, K., Karasaki, K., Marui, A., Uehara, H. and Nishikawa, N. 2009. Numerical investigation for the impact of CO_2 geologic sequestration on regional groundwater flow. *International Journal of Greenhouse Gas Control*, **3**, 586-599.

Yang, Y. and Aplin, A. C. 2009. A permeability–porosity relationship for mudstones. *Marine and Petroleum Geology*, doi:10.1016/j.marpetgeo.2009.07.001, pp 6.

Zhou, Q., Birkholzer, J. T., Tsang, C. and Rutqvist, J. 2008. A method for quick assessment of CO_2 storage capacity in closed and semi-closed saline aquifers. *International Journal of Greenhouse Gas Control*, **2**, 626-639.